Redox Biology 67 (2023) 102929

Contents lists available at ScienceDirect

Redox Biology

journal homepage: www.elsevier.com/locate/redox

Arginase2 mediates contrast-induced acute kidney injury *via* facilitating nitrosative stress in tubular cells

Ling-yun Zhou [a,1], Kun Liu [a,1], Wen-jun Yin [a], Yue-liang Xie [a], Jiang-lin Wang [a], Shan-ru Zuo [a], Zhi-yao Tang [a], Yi-feng Wu [a], Xiao-cong Zuo [a,b,*]

[a] Department of Pharmacy, The Third Xiangya Hospital, Central South University, Changsha, China
[b] Center of Clinical Pharmacology, The Third Xiangya Hospital, Central South University, Changsha, China

ARTICLE INFO

Keywords:
Contrast-induced AKI
Arginase2
Kidney tubular cells
Nitrosative stress
Apoptosis
Key target

ABSTRACT

Contrast-induced acute kidney injury(CI-AKI) is the third cause of AKI. Although tubular injury has been regarded as an important pathophysiology of CI-AKI, the underlying mechanism remains elusive. Here, we found arginase2(ARG2) accumulated in the tubules of CI-AKI mice, and was upregulated in iohexol treated kidney tubular cells and in blood samples of CI-AKI mice and patients, accompanied by increased nitrosative stress and apoptosis. However, all of the above were reversed in ARG2 knockout mice, as evidenced by the ameliorated kidney dysfunction and the tubular injury, and decreased nitrosative stress and apoptosis. Mechanistically, HO-1 upregulation could alleviate iohexol or ARG2 overexpression mediated nitrosative stress. Silencing and overexpressing ARG2 was able to upregulate and downregulate HO-1 expression, respectively, while HO-1 siRNA had no effect on ARG2 expression, indicating that ARG2 might inhibit HO-1 expression at the transcriptional level, which facilitated nitrosative stress during CI-AKI. Additionally, CREB1, a transcription factor, bound to the promoter region of ARG2 and stimulated its transcription. Similar findings were yielded in cisplatin- or vancomycin-induced AKI models. Taken together, ARG2 is a crucial target of CI-AKI, and activating CREB1/ARG2/HO-1 axis can mediate tubular injury by promoting nitrosative stress, highlighting potential therapeutic strategy for treating CI-AKI.

1. Introduction

Acute kidney injury (AKI), which affects approximately 13.3 million people around the world each year, has become a common and important public health problem [1,2]. Although once considered predominantly to be a self-limited and reversible condition, AKI is now recognized to be associated with high risk of non-recovery of kidney function, chronic kidney disease (CKD), and end-stage renal disease (ESRD) [3]. Contrast-induced AKI (CI-AKI) is the third leading cause of AKI [4,5], which occurs in up to 30 % of patients treated with iodine contrast media [6,7]. For old patients or those with diabetes, CKD, or hypertension, the prevalence of CI-AKI may be as high as 40 % [8], leading to high risk of in-hospital need for dialysis (<1 %), long-term kidney failure, and overall mortality (7 %–31 %) [8]. However, the mechanisms of CI-AKI are complex and there is no effective intervention for it. Therefore, it is essential to decipher the underlying mechanisms of CI-AKI to explore efficient preventive or therapeutic strategies.

The tubules, especially the proximal tubules, are exposed with potentially toxic drugs or their metabolites secreted into the tubular lumen [9]. Direct acute tubular injury has reported to be the main cause of CI-AKI [8]. Tubules are rich in mitochondria for the high energy demand [10]. Previous studies have found that contrast exposure can cause mitochondrial damage, renal tubular epithelial cells apoptosis, and renal injury [11,12]. Mitochondria-targeted protection can alleviate contrast-induced tubular cell death and acute kidney injury [13,14]. Our previous studies also found that mitochondrial permeability transition pore (mPTP) opening of tubular cells triggered mitochondrial dysfunction and tubular cells apoptosis in CI-AKI [15,16]. Thus, mitochondrial dysfunction of tubular cells may play a vital role in CI-AKI.

Arginase2 (ARG2), which is one of the two arginase isoforms, is reported to be highly expressed in the kidney localized to the mitochondria [17,18]. The physiological function of arginase is hydrolyzing L-arginine into urea and L-ornithine [19]. Defective function of arginase1 (ARG1), a hepatic arginase localized to the cytosol, could induce a toxic

* Corresponding author. Department of Pharmacy, The Third Xiangya Hospital, Central South University, Changsha, China.
E-mail address: zuoxc08@126.com (X.-c. Zuo).
[1] These authors made equal contributions to this work.

https://doi.org/10.1016/j.redox.2023.102929
Received 26 September 2023; Accepted 7 October 2023
Available online 10 October 2023

buildup of ammonia [20]. However, mice globally deficient in ARG2 were apparently indistinguishable from wide-type (WT) mice, and the physiologic role of ARG2 has not been well defined [21]. There is evidence showed that increased ARG2 activity seems to be involved in diabetic nephropathy by competing with nitric oxide synthase (NOS) for the same substrate, L-arginine, which results in reduced NO production and increased reactive nitrogen species [17,22]. A recent study also showed that the expression of ARG2 in the renal tubules of the cortex significantly increased after ischemia-reperfusion injury (IRI) and suppressing ARG2 could reduce nitrosative stress in the kidney [23]. And another study performed by Uchida et al., found that ARG2 promoted the inflammatory responses of macrophages, resulting in the exacerbation of cisplatin-induced AKI [24]. In contrast, Ansermet et al., reported that renal tubular ARG2 could attenuate kidney damage in IRI mice via participating in the formation of the corticomedullary urea gradient [25]. Thus, it is unclear whether ARG2 is detrimental or protective in AKI. What's more, the role and molecular mechanisms of ARG2 in CI-AKI have not been reported.

Consequently, the current experiments were performed to determine whether ARG2 is a key target of CI-AKI, and then investigate how ARG2 influences CI-AKI.

2. Materials and methods

2.1. Human subjects

We carried out present study in accordance with the Declaration of Helsinki (2008) of the World Medical Association, which was approval by the Third Xiangya Hospital Institutional Ethics Review Broad (#2021-S110, Changsha, China), following the Strengthening the Reporting of Observational Studies in Epidemiology (STROBE) recommendations for observational clinical trials. After screening for eligibility, we enrolled patients who were treated with contrast media and developed AKI at the Third Xiangya Hospital retrospectively. Those with known causes of AKI were excluded. AKI was diagnosed as an absolute increase of $\geq$26.5 μmol/L within 48 h or a relative increase of $\geq$50 % within 7 days in serum creatinine (SCr) [26]. Propensity score matching (1:1) was used to identify the controls who received contrast media without developing AKI by adjusting age, gender, diabetes mellitus, CKD, and chronic heart failure. Preoperative and postoperative (1–7 days after contrast media treatment) serum samples were collected to measure levels of SCr and ARG2. To avoid potential sources of bias, two well-trained operators independently collected the data, with the third operator resolving any disputes. The detailed characteristics of patients are shown in Supplementary Table S1.

2.2. Animals and treatment

Animal studies were approved by the Committee on the Ethics of Animal Experiments of Central South University and were performed in accordance with the National Institutes of Health Guidelines for the Care and Use of Laboratory. ARG2 knockout (KO) mice in the C57BL/6 background were purchased from the Cyagen Biosciences (Suzhou) Inc. Male WT C57BL/6 mice were purchased from the Department of Laboratory Animals of Central South University (Changsha, China). To induce CI-AKI mice model, male mice (6–8 weeks), which had undergone unilateral right nephrectomy 3 weeks before, were treated with water deprivation for 48 h, followed by intraperitoneal injection of furosemide (15 mL/kg). Thirty minutes later, iohexol (350 mg iodine/mL, GE Healthcare, China) was administrated (20 mL/kg) via tail vein. To induce cisplatin-induced AKI model, mice were intraperitoneal injected with a single dose of cisplatin (Sigma-Aldrich, P4394; 20 mg/kg). To induce vancomycin-induced AKI model, vancomycin (MedChemExpress, HY-17362; 500 mg/kg) was given to mice by intraperitoneal injection once a day for 7 days. Control mice experienced a similar procedure with an equal amount of saline instead of iohexol, cisplatin or vancomycin, respectively. We collected the blood samples and renal tissues 24 h after administration of iohexol or the last dose of vancomycin, and 72 h after cisplatin injection, respectively. Prior to administration of iohexol, the ARG inhibitor nor-NOHA (GLPBIO, GC10628; 100 mg/kg) or nitrosative stress inhibitor FeTPPS (Apexbio, GC10628; 30 mg/kg) was intraperitoneally injected once a day for three days.

2.3. Measurement of kidney function and injury

SCr and blood urea nitrogen (BUN) were measured to determine kidney function by the Third Xiangya Hospital clinical laboratory using automatic biochemistry analyzer (Hitachi 7600A, Japan). Formalin-fixed, paraffin-embedded left kidney tissues, which was stained with hematoxylin and eosin (HE), were used for renal histopathological evaluation. The tubular injury score was assessed using the following qualitative scoring system: 0, normal; 1, slight tubular injury with 0 %–10 % area affected; 2, moderate tubular injury with 11 %–25 % area affected; 3, significant tubular injury with 26 %–50 % area affected; 4, severe injury with 51 %–75 % area affected, and 5, high severe tubular injury with 76 %–100 % area affected [27].

2.4. Cell culture

Human kidney proximal tubular cells (HK-2 cells) were purchased from Zhong Qiao Xin Zhou Biotechnology Co., Ltd. Primary renal tubular cells were extracted as previously reported [28,29]. Kidneys were extracted from WT and ARG2 KO mice within 5 min after sacrifice, the cortex of kidneys were minced and incubated in 1 mg/mL collagenase II at 37 °C for 30 min. The collagenase was inactivated by adding the DMEM/F12 medium containing 10 % FBS. The digested renal tissue was first through a 100 μm filter, and then through a 70 μm and 40 μm filter (Corning). Filtrate was collected at the bottom of a 40 μm filter, centrifuged at 1000 r/min for 5 min, then inoculated in a culture bottle after medium suspension, and cultured until fusion. Cells were cultured in Dulbecco's modified Eagle's medium/F12 medium (DMEM/F12, Gibco, Thermo Fisher Scientific), which contained 10 % fetal bovine serum (Gibco, Thermo Fisher Scientific), 1 % penicillin (Gibco, Thermo Fisher Scientific), and 1 % streptomycin (Gibco, Thermo Fisher Scientific), in an incubator at 37 °C and of 5 % CO_2, until 70 % – 80 % confluent in 6- or 12- or 96- well multiwall plates before each experiment. To induce AKI cell models, cells were treated with iohexol (75 mg iodine/mL), cisplatin (2.5 μM), or vancomycin (4 mM) for 48 h, respectively. Nitrosative stress inhibitor FeTPPS (Apexbio, GC10628) was used at 100 μM 6 h before iohexol treatment. In some experiments, cells were treated with HO-1 agonist CoPP (Sigma, C1900) at 100 μM when exposed to iohexol. The Cell Counting Kit 8 (CCK8, Apexbio, Houston, USA) assay was used to detect cell viability in accordance with the manufacturer's instructions.

2.5. Gene silencing or overexpression

The siRNA of ARG2, HO-1, CREB1 and their matched scramble control were purchased from RiboBio Co., Ltd. (Guangzhou, China). In brief, cells were transfected with 100 nmol/L of the indicated siRNA using transfection reagent (RIBOBIO, China) according to the manufacturer's protocol. The sense sequence for ARG2 siRNA is '5-GAGGGCATATTGTCTATGA-3', for HO-1 siRNA is '5-CGATGGGTCCTTACACTCA-3', and for CREB1 siRNA is '5-GCTCGAGAGTGTCGTAGAA-3'. The ARG2 overexpression was achieved by transfection of PCDNA3.1-ARG2 expressing plasmid (Genechem, China) with Lipofectamine 3000 (Thermo Fisher Scientific, L3000015) according to the manufacturer's protocol.

2.6. Proteomic and transcriptomic

Proteomic and transcriptomic analyses of the kidneys of iohexol-

induced AKI mice were performed (12 mice, 6 mice in each group). Kidney tissue weighing 50 mg was lysed and homogenized. Following ultrasonic denaturation, 14 000 g were centrifuged for 15 min, with the supernatant then being filtered through a 0.22 m centrifuge tube to obtain the filtrate. After adding 20 g of protein to a 6× loading buffer solution and heating it to 100 °C for 5 min, it was electrophoresed using 12 % SDS-PAGE at 250 V for 40 min before being stained with Coomas bright blue. Each sample yielded an 80 g protein solution, which was then digested by enzymes and desalted in an ultrafiltration tube to produce peptide segments. The Easy- nLC system was used to separate the samples, and a Q Exactive Plus mass spectrometer was used to analyze them using mass spectrometry. The unlabeled quantitative calculation of proteomics data was carried out using the Label-free method of Maxquant. Lastly, and proteins were identified using the Uniprot MusMusculus-16998-20180905 database.

RNA was isolated after 50 mg of renal tissue was homogenized and lysed with Trizol. RNA Nano 6000 Assay Kit of the Bioanalyzer 2100 system and NanoPhotometer® spectrophotometer (IMPLEN, CA, USA) were used to assess the integrity and amount of RNA (Agilent Technologies, CA, USA). NEBNext® UltraTM RNA Library Prep Kit for Illumina® (NEB, USA) was used to generate sequencing libraries. After clustering, sequencing and analyzing, genes with an adjusted P value $<$ 0.05, found by DESeq2 R package (1.16.1), were considered to be significantly differentially expressed between groups.

2.7. Real-time polymerase chain reaction (RT-PCR)

Total RNA was separated and extracted from kidney tissues and renal tubular cells using Trizol reagent (TransGen Biotech, China), and the RT kit (TransGen Biotech, China) was used to reversely transcript RNA into cDNA according to the manufacturer's instructions. Then, real-time PCR was performed using SYBR green mixture kit and gene-specific primers. Target gene mRNA expression levels were determined by $2^{-\triangle\triangle Ct}$ technique and adjusted to β-actin.

2.8. Western blotting

Following primary antibodies were used in present study: anti-ARG2 (Cell Signaling Technology, #55003, 1:1000), anti-Casapse-3 (Cell Signaling Technology, #9662, 1:1000), anti-Bax (Abclonal, A0207, 1:1000), anti-Bcl-2 (Abclonal, A0208, 1:1000), anti-3-Nitrotyrosine (Bioss, bs-8551R, 1:1000), anti-HO-1 (Cell Signaling Technology, #43966, 1:1000), anti-P-CREB1 (Cell Signaling Technology, #9198, 1:1000), anti-CREB1 (Abclonal, A11989, 1:1000), anti-β-actin (Proteintech, 66009-1-Ig, 1:5000), and anti-β-Tubulin (Proteintech, 66240-1-Ig, 1:5000). Western blotting was performed, and band intensities were adjusted to internal control.

2.9. Immunofluorescence staining

The dewaxing solution and anhydrous ethanol were used to convert paraffin sections to water. After washing with PBS, 3 % BSA was used to block for 30 min later. Antigen repair solution was utilized for antigen repair. Primary antibody and fluorescein were incubated for night at 4 °C. After washing three times with PBS, the secondary antibody was added, incubating for 50 min at room temperature away from light. Add the DAPI dye solution and incubate at room temperature for 10 min without exposure to light after three PBS washes. After adding liquid B of the autofluorescence quencher, rinse for 10 min under running water. Seal for an anti-fluorescence pill. According to various fluorescence wavelengths, images were gathered using a fluorescence microscope. The following uses are made using antibodies and fluorescent dyes: anti-ARG2 (Bioss, bs-11397R), CD31 (Wuhan Servicebio Technology, GB11063-2), F4/80 (Wuhan Servicebio Technology, Q61549), Lotus Tetragonolobus Lectin (LTL) Fluorescein (Vector, FL-1321), Peanut Agglutinin (PNA) Fluorescein (Vector, FL-1071), Dolichos Biflorus Agglutinin (DBA) Fluorescein (Vector, FL-1031), DAPI (Wuhan Servicebio Technology, G1012). For cellular immunofluorescence, iohexol treated HK-2 cells were incubated with Mito-Tracker Red CMXRos for 30 min at 37 °C. After washing three times with PBS, the cells were fixed with 4 % paraformaldehyde fixative solution at 37 °C for 20 min, and then 0.3 % Triton X-100 at 4 °C for 20 min. Anti-ARG2 antibody (Bioss, bs-11397R; 1:100) was then added and incubated for 4 h. Add secondary antibody (diluted with 1%BSA) and incubate for 30 min at room temperature after washing with PBS. Anti-fluorescence quenching tablet sealing was done after the DAPI dye solution had been stained in the nucleus. Finally, confocal microscopy was used for photographic analysis (Leica).

2.10. Immunohistochemistry

After being uniformly coated with 3 % BSA, the dewaxed slices were sealed at room temperature for 30 min, and then incubated with the primary antibodies (anti-ARG2, Bioss, bs-11397R, 1:100; anti-3-Nitrotyrosine, Bioss, bs-8551R, 1:100) overnight at 4 °C. Tissue was covered with the secondary antibody that had been HRP-labeled after the sections had been PBS-washed. After that, it was incubated for 50 min at room temperature. Hematoxylin was used to stain the nucleus once more before being viewed under an optical microscope. The IHC Toolbox in Image J software was used to analyze the proportion of positive areas.

2.11. Enzyme-linked immunosorbent assay (ELISA)

After centrifuging the blood samples for 15 min at 4000 g, the serums were collected and kept at −80 °C. ARG2 ELISA kits (Shanghai Enzyme-linked Biotechnology Co., Ltd., YJ060179 and YJ002075) were used to detect the serum levels of ARG2 in mice and human using the diluted serum samples (1:50).

2.12. Terminal deoxynucleotidyl transferase dUTPnick-end labeling (TUNEL)

The paraffin-embedded tissue slide was deparaffinized and moisturized. After washing with distilled water, TUNEL kit was used to detect the apoptosis cells. A mixture of TDT enzyme, dUTP and buffer (1:5:50) was added to the slices, incubating for 2 h at 37 °C. Then, the slices were washed with PBS for three times and incubated with DAPI for 10 min at room temperature away from light. The anti-fade medium treated sections were then observed under fluorescence microscope.

2.13. Peroxynitrite measurement

Peroxynitrite assay kit (Abcam, ab233468) was used to detect the concentration of peroxynitrite. Cells were incubated with the Peroxynitrite Sensor Green working solution (10×) for 30 min at 37 °C away from light. After washing with PBS for three times, the hoechst 33342 dye solution was added, incubating for 10 min at room temperature. The Operetta® High Content Imaging System (PerkinElmer, Massachusetts, USA) was used to observe and measure the peroxynitrite [30,31].

2.14. Mitochondrial permeability transition pore (mPTP) assay

The mPTP assay kit (Beyotime Biotechnology, C2009S) was used to detect the mPTP opening. Cells were incubated with fluorescence quenching solution (100 μL/well) for 30 min, and then pre-warmed DMEM/F12 was used to instead the liquid for another 30 min at 37 °C away from light. The Operetta® High Content Imaging System (PerkinElmer, Massachusetts, USA) was used to observe and detect the mPTP [30,31].

2.15. Luciferase reporter assay

Cells was inoculated in 24-well culture plate, and then X-tremegene HP transfection solution (ROCHE) was used. A mixture of firefly luc plasmid, transcription factor plasmid, Renilla luc plasmid (0.5 μg; 0.5 μg; 0.02 μg), dissolving in 100 μL of opti-MEM, was added to each well. After adding the plasmid and X-tremegene HP mixture, cells were incubated for 6 h. Then, complete medium with 10 % serum as a supplement was used to instead the mixture, and cells were gathered for luciferase detection 48 h after transfection using the Dual-Luciferase® Reporter Assay System (Promega, E1910, USA).

2.16. ChIP-PCR assay

The enrichment of CREB1 to the promoter region of ARG2 in HK-2 cells was assessed using a ChIP-PCR experiment. HK-2 cells were gathered and connected with 1 % formaldehyde for 10 min at room temperature. Centrifugation was followed by the addition of lysis buffer and 30 min at 4 °C. After that, 5 min of ultrasonic crushing was performed. The 1 μg supernatant was used as the input and stored at 4 °C. 5 μg samples were incubated at 4 °C overnight with IgG antibody (Invitrogen, 11203D) or CREB1 antibody (Abclonal, A11989), respectively. Protein G Magnetic Beads were added to the IP sample, which was then incubated at 4 °C for 4 h. Separate magnetic beads and wash thoroughly. RNase was then added, with the final concentration being 1 μg/mL, and the mixture was heated at 65°C for 2 h before being incubated at 37°C for 20 min. A PCR purification kit (Qiagen 28106) was used for the purification process. The DNA was detected using RT-PCR and agarose gel electrophoresis (AGE) methods to identify the purified samples. Following is the primer sequence: ChIP-ARG2-F:'5-CGTGAAGATTGGTGTCGGCT-3'; ChIP-ARG2-R: '5-GACGCCAGAAGGCCAATATC-3'.

2.17. Statistical analysis

Data were presented as mean ± SD. Student *t*-test was used to compare the differences between two groups. One-way analysis of variance (ANOVA), two-way ANOVA, and three-way ANOVA were used to compare the differences among multiple-groups when needed plus Tukey's post-test, respectively. Statistical analyses were performed using GraphPad Prism 9.0. Statistically significant differences were defined as a 2-tailed value of $P < 0.05$.

3. Results

3.1. ARG2 accumulates in the kidneys of CI-AKI mice and is upregulated in blood samples of CI-AKI mice and patients

To identify the key target of CI-AKI, we utilized iohexol-induced AKI as a representative model and employed proteomics and transcriptomics techniques to analyze protein and mRNA alterations in the kidneys of mice. Iohexol induced a significant increase in SCr, BUN, and tubular injury score at 24 h after iohexol treatment compared with those of control mice (Figs. S1A–S1D). And results of proteomics and transcriptomics showed that both mRNA and protein expressions of ARG2 significantly increased in the kidneys of iohexol-induced AKI mice (Fig. 1A and B), which was further verified by western blotting (Fig. 1C and D), RT-PCR (Fig. 1E), and immunohistochemistry staining also showed that ARG2-positive staining significantly increased in renal tubules of mice after iohexol treatment (Fig. 1F). Next, the localization of ARG2 in the kidneys was studied. As determined by confocal immunofluorescence using tubular (LTL, proximal tubule; PNA, distal tubule; DBA, collecting duct), endothelial (CD31), and macrophage (F4/80) markers, the ARG2 extensively colocalized with tubules in the CI-AKI mice models (Fig. 1G), indicating the accumulation of ARG2 in renal tubules after iohexol treatment, especially in the proximal tubules.

The upregulated ARG2 expression observed *in vivo* was corroborated in the *in vitro* experiments. After treating primary renal tubular cells and HK-2 cells with 75 mg(I)/mL iohexol for 0 h–48 h, ARG2 mRNA and protein levels significantly increased in a time-dependent manner, elevating at 6 h, and lasting at least 48 h (Fig. 1H–J, Figs. S2A–S2C). As ARG2 was previously reported to localize to mitochondria [23], we performed double staining of mitochondria with Mito-Tracker Red CMXRos and ARG2. Results showed that there was obvious colocalization between ARG2 and mitochondria in the control group, and the mitochondrial fluorescence and the colocalization between ARG2 and mitochondria decreased significantly due to iohexol (Fig. 1K). To determine whether the other isoform of ARG, ARG1, is upregulated in CI-AKI, western blotting was performed, and results showed that ARG1 was not increased in the HK-2 cell after iohexol treatment (Fig. S3A).

Of interest is that serum level of ARG2 in CI-AKI mice was found to be significantly increased (Fig. 1L). In addition, we measured ARG2 in human serum samples with or without CI-AKI. The level of serum ARG2 was also significantly higher in the CI-AKI patients who received contrast media when compared with the matched non-CI-AKI individuals (Fig. 1M). Detailed clinical characteristics of patients were shown in Table S1.

Thus, iohexol could significantly upregulate mRNA and protein expressions of ARG2 in the kidneys of mice, mainly localizing to mitochondria of renal tubular cells, which was also increased in the blood samples of CI-AKI mice and patients.

3.2. ARG2 deficiency attenuates iohexol-induced kidney injury and apoptosis

To explore the role of ARG2 in CI-AKI, we firstly used the unselective ARG inhibitor, nor-NOHA, to investigate whether ARG inhibition could protect against CI-AKI. Results showed that nor-NOHA markedly blunted the elevation in SCr, BUN and tubular injury score (Fig. 2A–C) when compared with those received an equal amount of saline. HE staining revealed that the renal tubule vacuolar degeneration was significantly increased in mice induced by iohexol, and nor-NOHA intervention could significantly reduce the tubular vacuolar degeneration (Fig. 2D). Then, we generated ARG2 KO mice. ARG2 protein expression was significantly lower in the renal tissues of ARG2 KO mice compared with WT mice even when exposed to iohexol (Fig. S3B), while ARG1 expression was not induced in a compensatory manner in the kidneys of ARG2 KO mice (Fig. S3C). Under basal conditions, ARG2 KO mice were viable with no detectable defect in renal structure or function (Fig. 2E−H), and the levels of SCr (Fig. 2E) and BUN (Fig. 2F) were both remarkably reduced in iohexol treated ARG2 KO mice when compared with similarly treated WT mice as well as decreased pathologic injury scores (Fig. 2G) and alleviated renal tubular vacuolar degeneration (Fig. 2H), indicating that ARG2 ablation is beneficial for CI-AKI.

Next, both of TUNEL staining and protein expressions of cleaved caspase-3, Bax and Bcl-2 were used to detect apoptosis, which has been demonstrated to play a key role in CI-AKI. As shown in Fig. 3A–F, compared with the WT mice, iohexol induced increases in TUNEL-positive cells (Fig. 3A and B) and protein expressions of cleaved caspase-3 (Fig. 3C and D) and Bax (Fig. 3C and F), and the decrease in protein expression of Bcl-2 (Fig. 3C and E) were significantly alleviated in kidneys of ARG2 KO mice.

The above *in vivo* results were replicated in cells transfected with ARG2 siRNA or ARG2 overexpression plasmid, respectively. In primary renal tubular cells extracted from ARG2 KO mice kidneys, iohexol-induced ARG2 mRNA expression upregulation and decrease in cell viability were found to be alleviated when compared with those extracted from WT mice kidneys (Figs. S3D and S3E). Similarly, iohexol-induced protein expression of ARG2 could be reversed by transfecting ARG2 siRNA in HK-2 cells (Fig. 3G and H). In the meanwhile, ARG2 siRNA markedly reduced the percentage of TUNEL-positive apoptotic cells, and alleviated iohexol-induced increases in protein expressions of

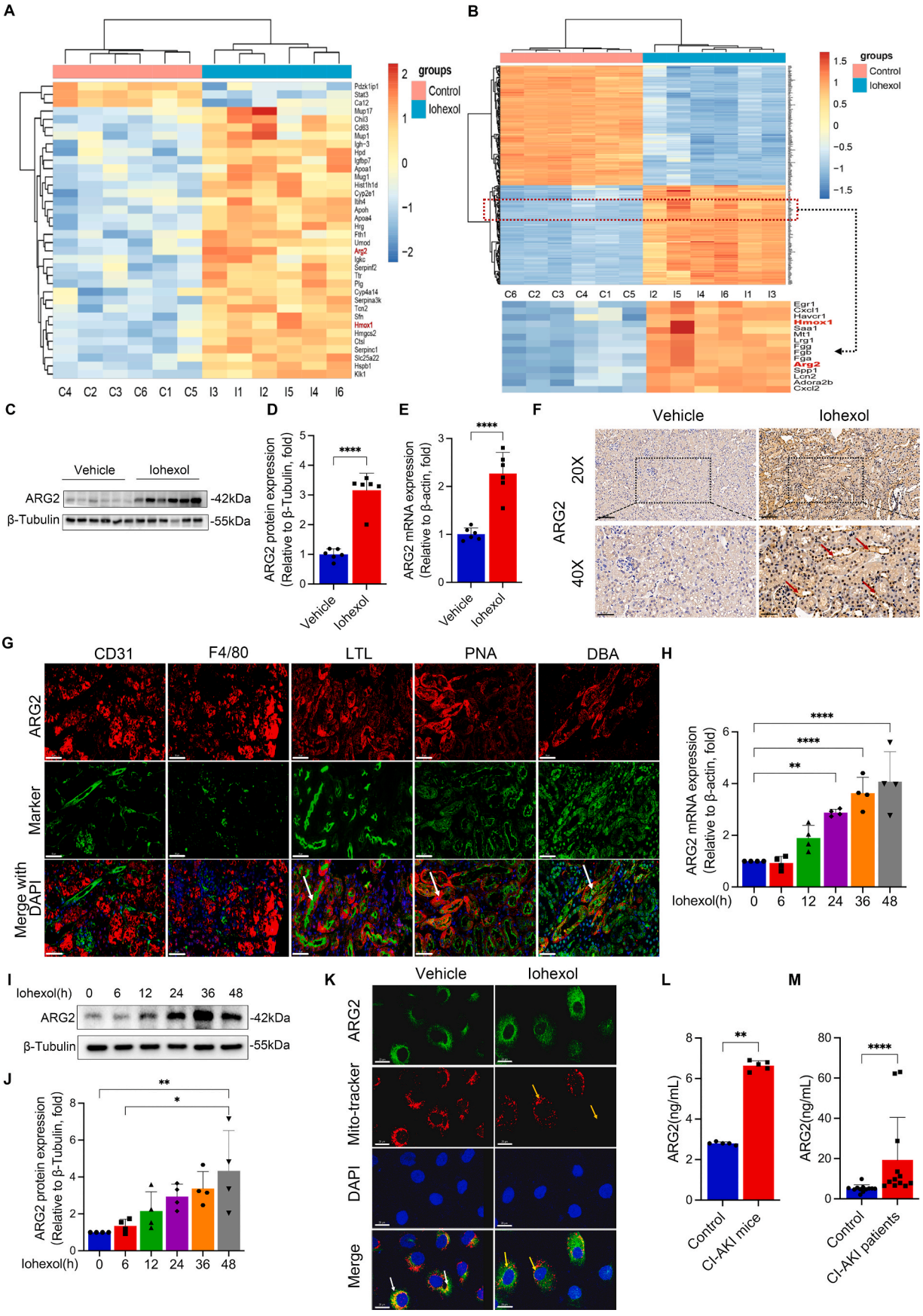

(caption on next page)

Fig. 1. ARG2 is upregulated in the CI-AKI mice kidneys and primary tubular epithelial cells, and increased in blood samples of CI-AKI mice and patients. (A) Heat map of proteomics in iohexol-induced AKI mice. *P-Value* <0.05 and log2 fold change (FC) > 2. (B) Heat map of transcriptomics in iohexol-induced AKI mice. *P-Value* <0.0001 and log2 fold change (FC) > 3. (C–E) The ARG2 protein and mRNA expressions were evaluated in the kidneys of mice treated with iohexol. (F) Representative images of immunohistochemistry staining of ARG2 in the kidneys of iohexol-induced AKI mice. The red arrows indicate deeper ARG2-positive staining of renal tubules. Scale, 20×, 100 μm, 40×, 50 μm. (G) Representative images of the immunofluorescence colocalization of CD31, F4/80, LTL, PNA, and DBA with ARG2 in the kidney of iohexol-induced AKI mice. The following specific markers were used: endothelial, CD31; macrophage, F4/80; proximal tubule, lotus tetragonolobus lectin (LTL); distal tubule, peanut agglutinin (PNA); and collecting duct, dolichos biflorus agglutinin (DBA). The white arrows indicate positive tubules with colocalization of ARG2 and specific tubular markers. Scale, 50 μm. (H–J) ARG2 protein and mRNA expressions in primary tubular epithelial cells treated with iohexol. (K) Representative image of ARG2 and mito-tracker immunofluorescence colocalization in HK-2 cells. The orange arrows indicate that iohexol causes a decrease in mitochondrial fluorescence. The white arrows indicate the normal colocalization of ARG2 with mitochondria. The yellow arrows indicate that iohexol leads to reduced colocalization of ARG2 with mitochondria. Scale, 20 μm. (L and M) Serum levels of ARG2 in CI-AKI mice (L) and patients (M). $^{*}P < 0.05$, $^{**}P < 0.01$, $^{***}P < 0.001$, $^{****}P < 0.0001$. mean ± SD, n = 5-6 in mice, n = 3–6 in HK-2 cells.

cleaved caspase-3 and Bax, and decrease in protein expression of Bcl-2 in HK-2 cells (Fig. 3I–K). In contrast, transfecting with ARG2 overexpression plasmid could further increase iohexol-induced ARG2 protein expression in HK-2 cells Fig. S4A, and decreased the cell viability (Figs. S4A and S4B).

Collectively, above findings demonstrate that the elevation of ARG2 mediated iohexol-induced renal dysfunction, tubular injury, and apoptosis in CI-AKI.

3.3. ARG2 mediates tubular apoptosis through nitrosative stress during CI-AKI, which may be not relevant to the NOS

As ARG2 was implicated in the regulation of reactive nitrogen species, we speculated that the upregulation of ARG2 in the kidneys mediated nitrosative stress, then leading to the tubular apoptosis during CI-AKI. To verify the role of nitrosative stress in CI-AKI, we utilized the specific peroxynitrite decomposition catalyst, FeTPPS, to scavenge reactive nitrogen species and alleviate nitrosative stress. As shown in Fig. 4A–D, the histologic damage and renal dysfunction induced by iohexol were markedly attenuated by FeTPPS. Furthermore, iohexol-induced increased level of $ONOO^{-}$ (Fig. 4E and F) and protein expression of 3-nitrotyrosine (3-NT) (Fig. 4G and H), the marker of nitrosative stress, and the upregulated cleaved caspase-3 protein expression (Fig. 4G and I), which detects apoptosis, were significantly reversed by FeTPPS treatment in HK-2 cells. All of the above results confirmed the role of nitrosative stress in iohexol-induced AKI.

We subsequently assessed the contribution of ARG2 in nitrosative stress during CI-AKI. In CI-AKI mice models, the 3-NT protein expression in renal tissues of ARG2 KO mice were much lower than that in similarly treated WT mice as determined by western blotting and histochemical staining analyses (Fig. 5A–D), indicating that ARG2 ablation is beneficial for reducing the nitrosative stress in CI-AKI. The above *in vivo* results were replicated in cells. The increase in protein expression of 3-NT (Fig. 5E and F) and the $ONOO^{-}$ production (Fig. 5G and H) induced by iohexol were significantly reduced in ARG2 siRNA transfected HK-2 cells compared with those transfected with scramble siRNA. Similar results were found in iohexol treated primary tubular cells extracted from WT mice kidneys and ARG2 KO mice kidneys (Figs. S5A, S5B, S5D and S5E), and even when HK-2 cells were cultured in L-arginine-free medium (Fig. S6), which confirmed the role of ARG2 in mediating nitrosative stress during CI-AKI. Because the colocalization of ARG2 and mitochondria, the effect of ARG2 siRNA on iohexol-induced mitochondrial injury was also evaluated, and results showed that iohexol-induced mPTP opening significantly recovered in cells transfected with ARG2 siRNA (Fig. S7).

To more clearly examine whether NOS, which competes with ARG for the same substrate, is involved in the ARG2 mediated nitrosative stress, we detected the protein expressions of three isoforms of NOS, iNOS, nNOS and eNOS. The most prominent NOS isoform in renal tubular cells was demonstrated to be iNOS. However, neither iohexol nor ARG2 siRNA changed the protein expression of any isoforms of NOS (Fig. S8).

All the above results suggest that ARG2 mediates nitrosative stress and subsequent apoptosis during CI-AKI, which may be not relevant to NOS.

3.4. ARG2 inhibits transcription and expression of HO-1, facilitating nitrosative stress during CI-AKI

To elucidate the potential mechanism responsible for ARG2 mediated nitrosative stress in CI-AKI, we examined the correlations between all differentially expressed proteins [32] measured by proteomics of iohexol induced AKI mice kidneys compared with the control group. After the analysis, HO-1 which was demonstrated to have a significantly negative correlation with ARG2, caught our attention (Fig. 6A). As an anti-nitrosative stress factor, HO-1 mRNA and protein expressions were significantly increased in mice treated with iohexol (Fig. 6B–D), which may protect against iohexol-induced AKI. No matter in primary tubular cells (Fig. 6E–G) or in HK-2 cells (Figs. S9A-S9C), the expressions of HO-1 protein (24 h) and mRNA (6 h) increased at the early stage of iohexol treatment, but decreased significantly after a long period of treatment (48 h), which was in contrast to the continuous increase of ARG2 after iohexol treatment. Next, we investigated the potential effect of HO-1 on CI-AKI. HO-1 silencing (Figs. S9D and S9E) significantly aggravated iohexol induced cell death (Fig. S9F), while activating HO-1 using the HO-1 agonist, CoPP, was able to significantly alleviate the iohexol-induced mPTP opening (Figs. S9G and S9H) and decrease in cell viability (Fig. S9I). Additionally, HO-1 overexpression was able to reverse iohexol or ARG2 overexpression induced nitrosative stress (Fig. 6H–K) and decreased cell viability (Fig. S9J) in HK-2 cells, suggesting that HO-1 may be a key downstream target involved in ARG2 mediated nitrosative stress and cell death during CI-AKI.

Based our hypothesis that the upregulated protein expression of ARG2 might inhibit the expression of HO-1, we firstly tested whether protein expression of HO-1 was altered by the upregulating or downregulating of ARG2. Both iohexol treatment and ARG2 KO markedly increased HO-1 protein expression in mice kidneys (Fig. 6C and D). Consistent with the findings *in vivo*, in primary renal tubular cell extracted from ARG2 KO mice kidneys, iohexol-induced HO-1 protein expression downregulation was found to be alleviated when compared with those extracted from WT mice kidneys (Figs. S5A and S5C). Further, silencing ARG2 significantly increased iohexol suppressed protein expression of HO-1 in HK-2 cells (Fig. 7A and C), while overexpressing ARG2 significantly decreased HO-1 protein expression no matter with or without iohexol treatment (Fig. 7B and D). In the meanwhile, a higher HO-1 mRNA level was discovered in HK-2 cells treated with ARG siRNA compared with those exposed to iohexol at 0 h, 12 h (Fig. 7E), but a lower HO-1 mRNA level was discovered in HK-2 cells treated with ARG2 overexpression plasmid compared with those exposed to iohexol at 0 h, 12 h, 24 h and 48 h (Fig. 7F). However, HO-1 siRNA or CoPP could not affect the iohexol-induced ARG2 protein expression (Fig. 7G–J). We further investigated whether ARG2 promoted the protein degradation of HO-1 using cycloheximide (CHX, an inhibitor of protein synthesis). Results showed that HO-1 degradation was not slowed by ARG2 silencing under CHX treatment, suggesting that ARG2 does not decrease HO-1 levels by promoting degradation of HO-1

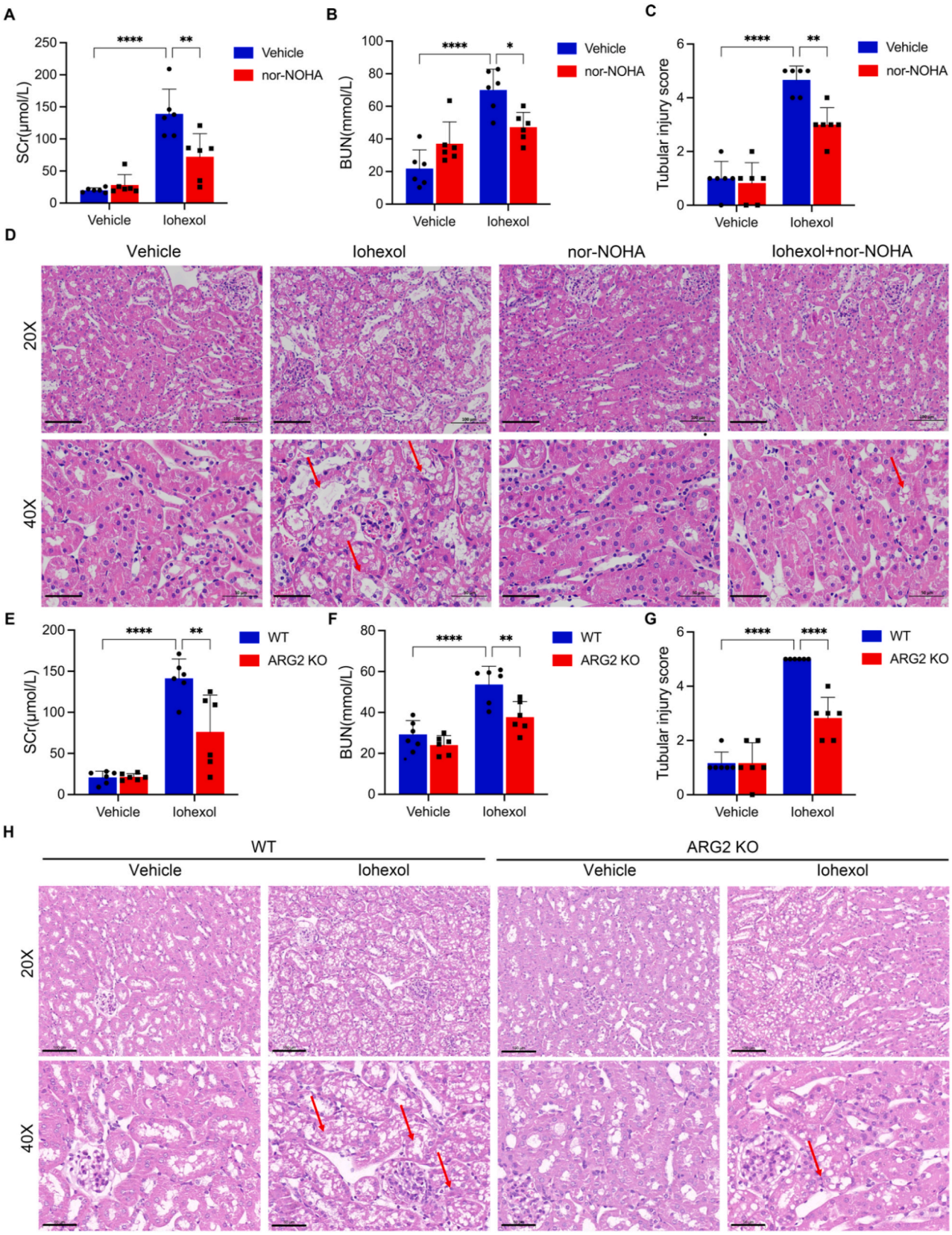

Fig. 2. ARG2 inhibition and deficiency significantly ameliorate iohexol-induced AKI. (A–D) Renal function and renal tissue injury of iohexol-induced AKI mice treated with nor-NOHA were assessed by SCr, BUN, and tubular injury score. Scale, 20×, 100 μm, 40×, 50 μm. (E–H) Renal function and renal tissue injury of ARG2 KO and WT mice injected by iohexol via tail vein were assessed by SCr, BUN, and tubular injury score. The red arrows indicate the vacuolar degeneration of renal tubules. Scale, 20×, 100 μm, 40×, 50 μm $^{*}P < 0.05$, $^{**}P < 0.01$, $^{***}P < 0.001$, $^{****}P < 0.0001$. mean ± SD, n = 6.

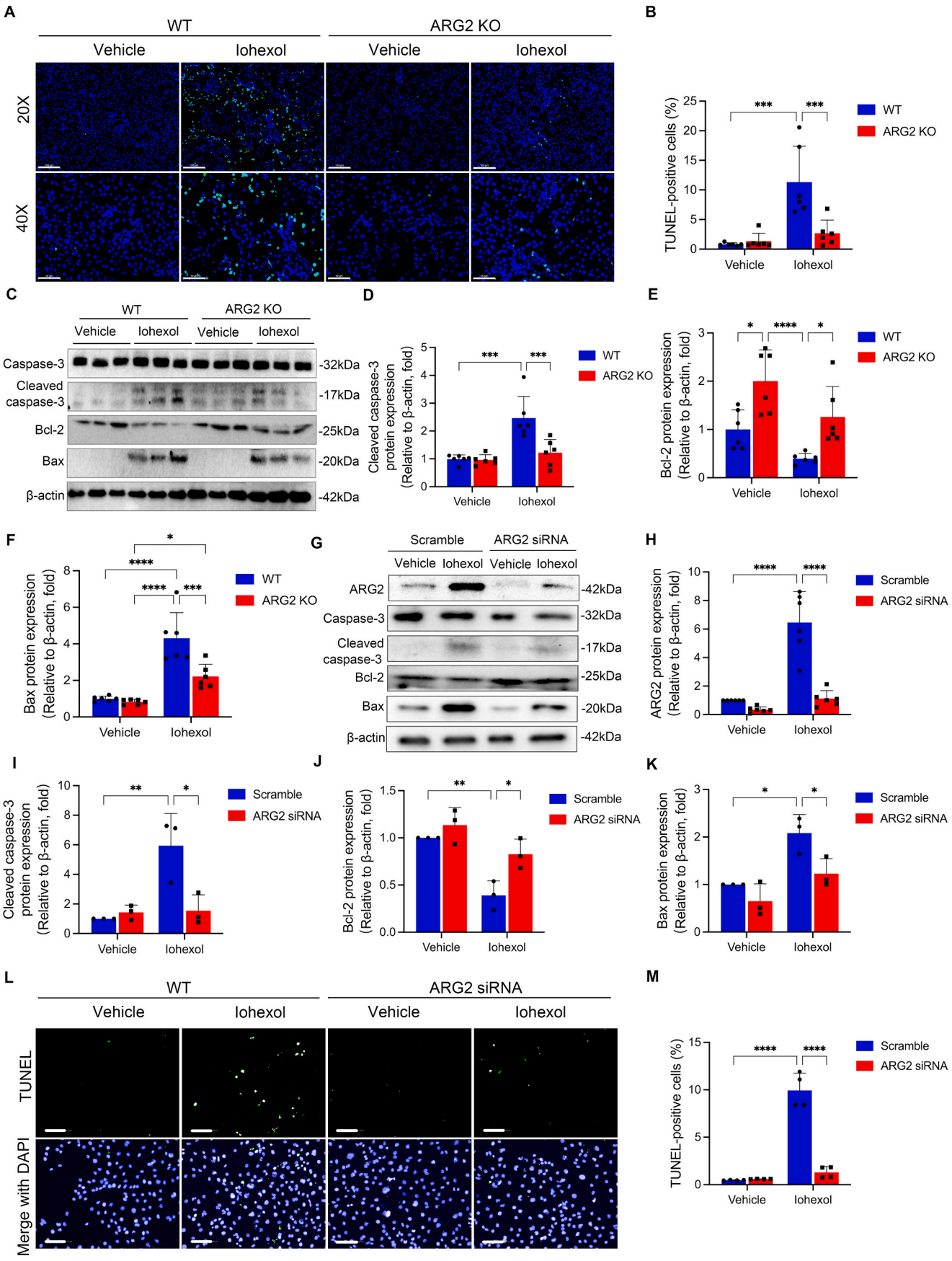

(caption on next page)

Fig. 3. ARG2 deficiency significantly reduces apoptosis in iohexol-induced AKI mice and HK-2 cells. (A and B) Representative images of TUNEL staining in ARG2 KO and WT mice treated with iohexol. TUNEL-positive cells and nuclei were indicated by green and blue fluorescence, respectively. (C–F) The protein expressions of caspase-3, cleaved caspase-3, Bcl-2, and Bax were evaluated with western blotting in ARG2 KO and WT mice administrated with iohexol. β-actin was used as the loading control. (G–K) Western blotting was used to evaluate the protein expressions of ARG2, caspase-3, cleaved caspase-3, Bcl-2, and Bax in HK-2 cells transfected with ARG2 siRNA and incubated with iohexol. (L and M) TUNEL staining was performed to examine apoptotic HK-2 cells transfected with ARG2 siRNA and incubated with iohexol. TUNEL-positive cells and nuclei were indicated by green and blue fluorescence, respectively. $^{*}P < 0.05$, $^{**}P < 0.01$, $^{***}P < 0.001$, $^{****}P < 0.0001$. mean ± SD, n = 6 in mice, n = 3-6 in HK-2 cells.

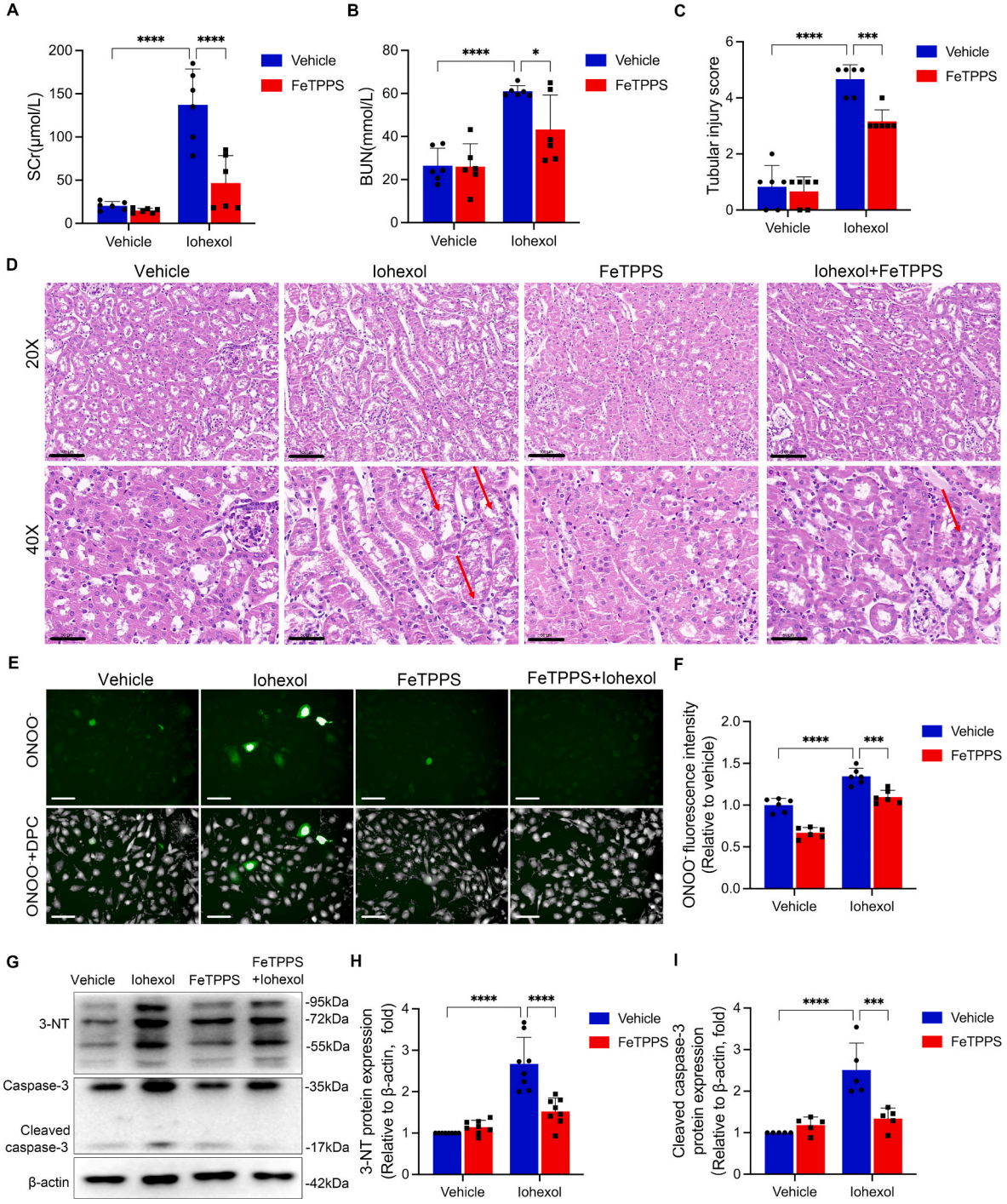

Fig. 4. FeTPPS rescues nitrosative stress caused by iohexol in mice and HK-2 cells. (A–D) Renal function and renal tissue injury of AKI mice induced by iohexol treated with or without FeTPPS were assessed by SCr, BUN, and tubular injury score. The red arrows indicate the vacuolar degeneration of renal tubules. (E and F) The level of $ONOO^{-}$ was evaluated with immunofluorescence in HK-2 cells cultured with FeTPPS and iohexol. Green fluorescence indicates $ONOO^{-}$. The number of cells was counted by DPC. DPC, Digital phase contrast. Scale, 100 μm. (G–I) The protein expressions of 3-NT, caspase-3 and cleaved caspase-3 were evaluated by western blotting in HK-2 cells cultured with FeTPPS and iohexol. $^{*}P < 0.05$, $^{**}P < 0.01$, $^{***}P < 0.001$, $^{****}P < 0.0001$. mean ± SD, n = 6 in mice, n =5-8 in HK-2 cells.

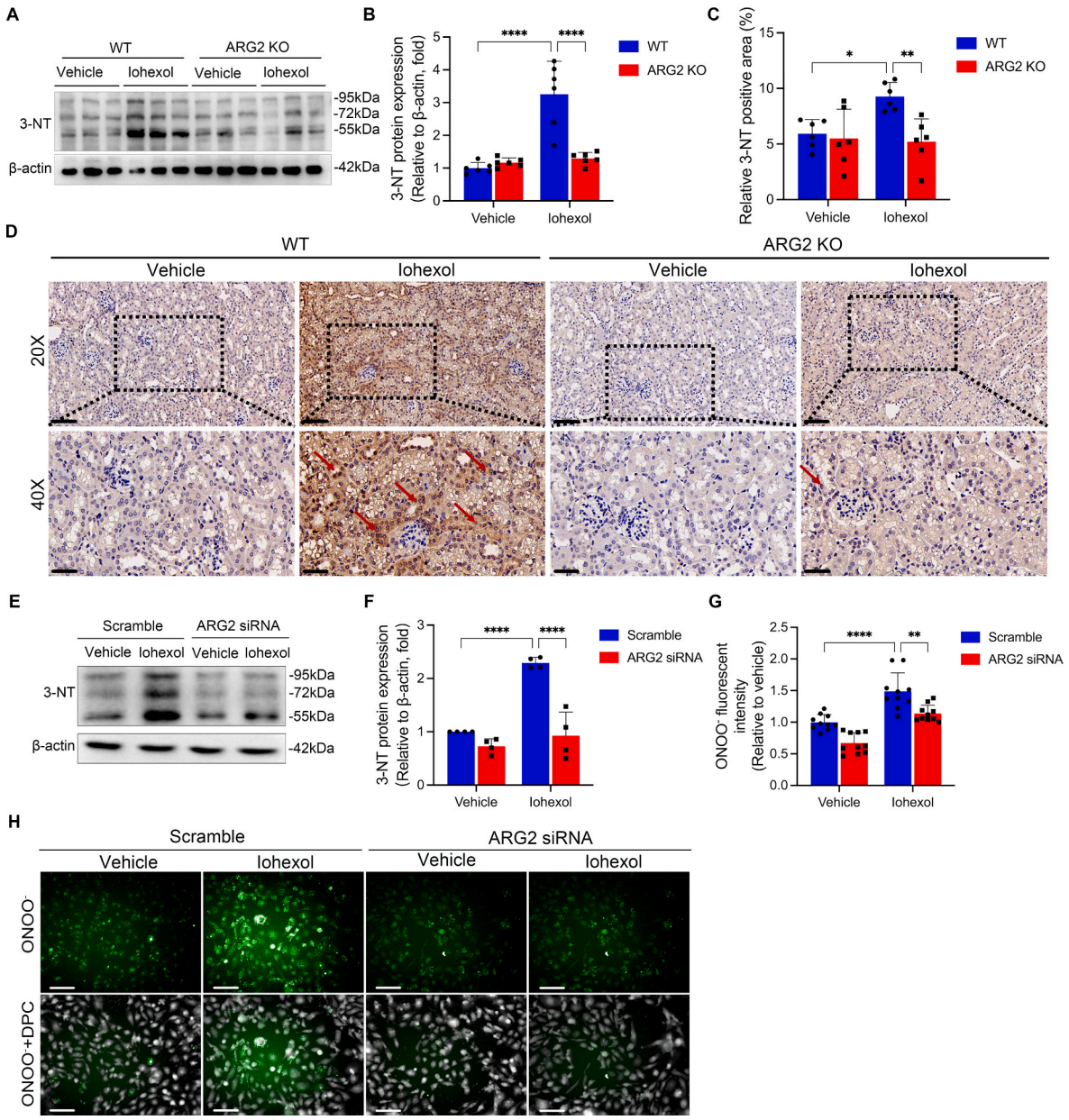

Fig. 5. ARG2 mediates nitrosative stress in iohexol-induced AKI and HK-2 cells. (A and B) The protein expression of 3-NT was evaluated by western blotting in ARG2 KO and WT mice treated with iohexol. (C and D) Representative images of immunohistochemistry staining of 3-NT in the kidneys of ARG2 KO and WT mice treated with iohexol. The red arrows indicate deeper 3-NT-positive staining of renal tubules. Scale, 20×, 100 μm, 40×, 50 μm. (E and F) The expression of 3-NT was evaluated with western blotting in HK-2 cells transfected with ARG2 siRNA and incubated with iohexol. (G and H) The level of $ONOO^-$ was evaluated with immunofluorescence in HK-2 cells transfected with ARG2 siRNA and incubated with iohexol. Green fluorescence indicates $ONOO^-$. The number of cells was counted by DPC. DPC, Digital phase contrast. Scale, 100 μm $^*P < 0.05$, $^{**}P < 0.01$, $^{****}P < 0.0001$. mean ± SD, n = 6 in mice, n = 3-10 in HK-2 cells.

(Fig. 7K and L). Taken together, ARG2 may inhibit HO-1 expression at the transcriptional level, which facilitates nitrosative stress during CI-AKI.

3.5. cAMP responsive element binding protein 1 (CREB1) promotes ARG2 transcription

As the limited information about the factors that contribute to ARG2 upregulation following injury, we conducted the bioinformatics analysis to determine the transcription factors that might regulate ARG2 expression. And we found that CREB1 had 26 binding sites in the promoter region of ARG2 (Table S2). Luciferase reporters assay and ChIP further verified that CREB1 targeted promoter sites of ARG2 (Fig. 8A and B). What's more, we observed significant induction in the phosphorylation of CREB1 as early as 6 h, in both renal tissues of mice (Fig. 8C and D) and HK-2 cells (Fig. 8E and F) treated with iohexol. Following transfection with CREB1 siRNA, the ARG2 protein expression was significantly downregulated in HK-2 cells, even under iohexol treatment (Fig. 8G–J). However, overexpressing ARG2 could not affect the CREB1 protein expression (Fig. 8K and L). All the above results indicate that CREB1 may promote ARG2 transcription, responsible for the increased ARG2 protein expression in CI-AKI.

3.6. ARG2 may be a potential common target of cisplatin-, or vancomycin-induced AKI

To further investigate whether ARG2 is a crucial target of other drugs induced AKI, we used cisplatin or vancomycin, two clinical commonly

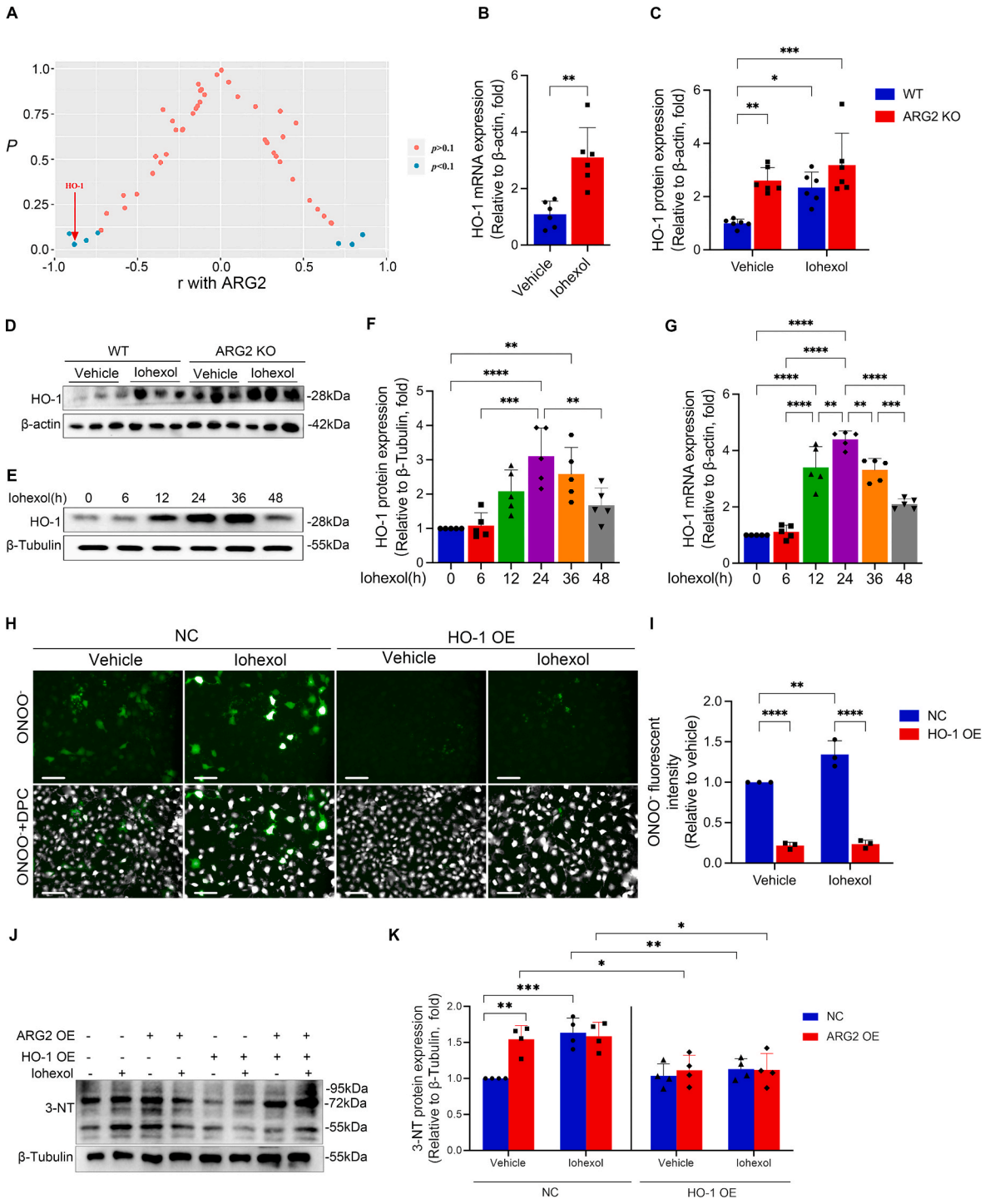

Fig. 6. HO-1 is involved in ARG2 mediated nitrosative stress. (A) Correlation between ARG2 protein expression and significantly different proteins of proteomics. X-axis, R with ARG2; Y-axis, *P*-value. (B) The HO-1 mRNA expression was evaluated in mice treated with iohexol. (C and D) The HO-1 protein expression was evaluated by western blotting in ARG2 KO and WT mice administrated with iohexol. (E–G) The HO-1 mRNA and protein expressions were evaluated in primary tubular epithelial cells incubated with iohexol. (H and I) The level of $ONOO^-$ was evaluated by immunofluorescence in HK-2 cells transfected with HO-1 overexpression plasmid or cultured with iohexol. Green fluorescence indicates $ONOO^-$. The number of cells was counted by DPC. DPC, Digital phase contrast. Scale, 100 μm. (J and K) The 3-NT protein expression was evaluated by western blotting in HK-2 cells incubated with iohexol and transfected with ARG2 overexpression plasmid and HO-1 overexpression plasmid. $^*P < 0.05$, $^{**}P < 0.01$, $^{***}P < 0.001$, $^{****}P < 0.0001$. mean ± SD, n = 6 in mice, n = 3-6 in cells.

used medications, to establish AKI mice (Figs. S1E-S1L) and cell models, and confirmed the renal accumulation of ARG2 via western blotting (Fig. 9A and B, Fig. 10A and B), RT-PCR (Fig. 9C and 10C), and immunohistochemistry staining (Fig. 9D and 10D). Also, the localization of ARG2 in the proximal tubules were found by immunofluorescence colocalization in both cisplatin-(Fig. 9E) and vancomycin- (Fig. 10E) induced AKI mice kidneys. And upregulated ARG2 protein expression was confirmed in primary renal tubular cells treated with cisplatin (Fig. 9F and G) or vancomycin (Fig. 10F and G).

What's more, similar protective effects of ARG2 deficiency were found in cisplatin- or vancomycin-induced AKI mice models, as evidenced by the remarkably reduced levels of SCr and BUN (Fig. 9H and I,

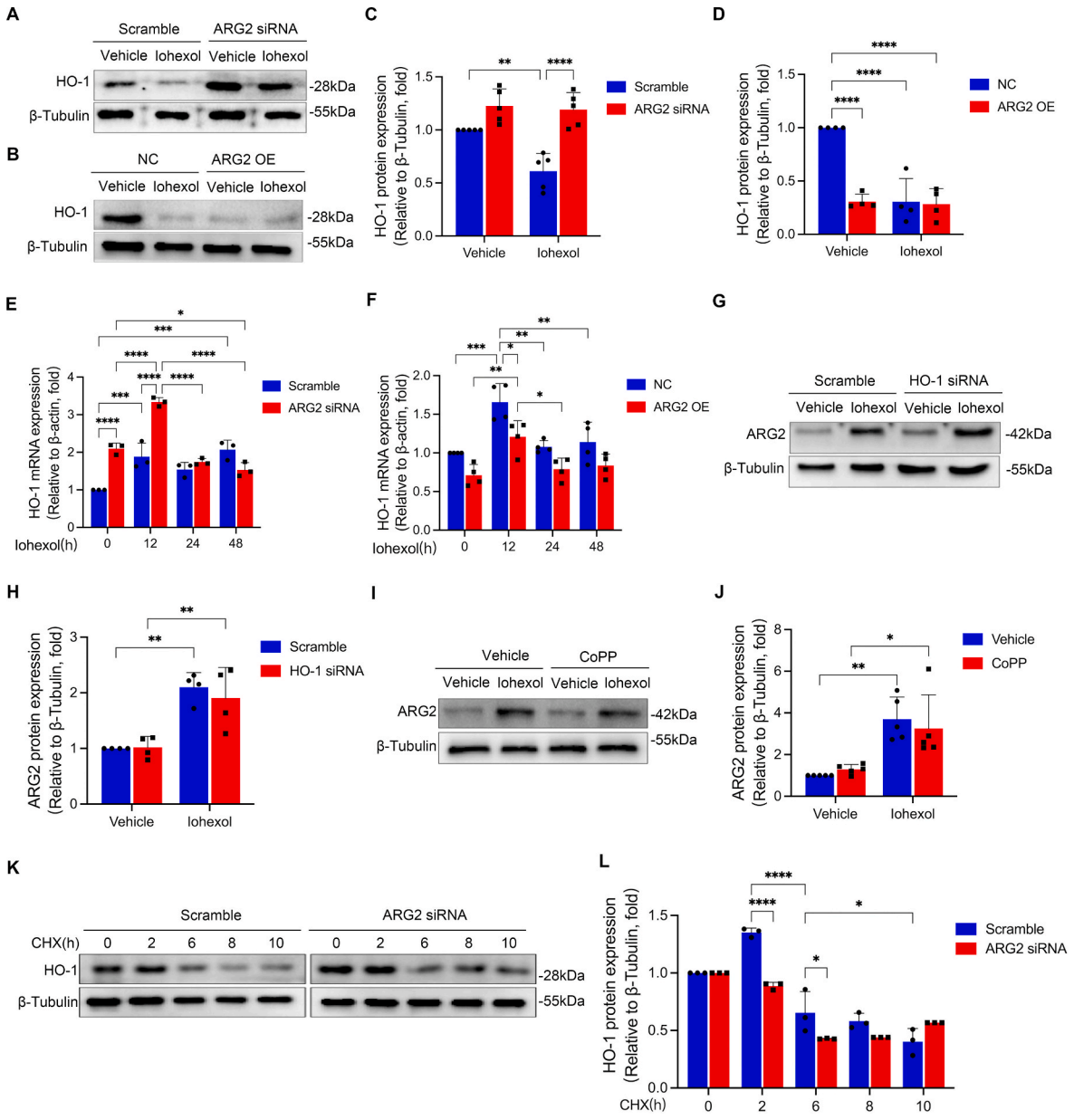

Fig. 7. ARG2 inhibits the expression of HO-1 at the transcriptional level in HK-2 cell cultured with iohexol. (A–D) The HO-1 protein expression was examined by western blotting in HK-2 cells transfected with ARG2 siRNA or ARG2 overexpression plasmid, and incubated with iohexol. (E and F) The HO-1 mRNA expression was evaluated in HK-2 cells transfected with ARG2 siRNA or ARG2 overexpression, and incubated with iohexol. (G and H) The ARG2 protein expression was evaluated with western blotting in HK-2 cells transfected with HO-1 siRNA or cultured with iohexol. (I and J) The ARG2 protein expression was evaluated with western blotting in HK-2 cells cultured with CoPP and iohexol. (K and L) The HO-1 protein expression was evaluated with western blotting in HK-2 cells transfected with ARG2 siRNA or cultured with CHX. $^{*}P < 0.05$, $^{**}P < 0.01$, $^{***}P < 0.001$, $^{****}P < 0.0001$. mean ± SD, n = 3-6 in HK-2 cells.

Fig. 10H and I), and decreased pathologic injury scores when compared with similarly treated WT mice (Fig. 9J and K, Fig. 10J and K). Similar to the iohexol-induced AKI model, the expression of HO-1 protein was also increased in ARG2 KO mice or cisplatin- or vancomycin-induced AKI mice kidneys (Fig. 9L and M, Fig. 10L and M). Thus, ARG2 ablation is also beneficial for cisplatin- or vancomycin-induced AKI, indicating that ARG2 may be a potential common target of those drugs induced AKI. However, further studies are needed to confirm the assumption.

4. Discussion

CI-AKI is one of the most common causes of AKI, which was previously perceived as a self-limited condition but now known to be associated with progression to CKD, sustained functional impairment and death. However, the medical intervention is not effective enough to prevent the occurrence of AKI or improve the long-term outcomes of AKI for the unclear underlying pathophysiology [33]. ARG2 has been reported to be involved in a variety of pathological processes, including oxidative stress, apoptosis, and inflammation [34]. Nevertheless, little is known about the role of ARG2 in CI-AKI. In present study, we found that ARG2 is highly expressed in the kidneys of CI-AKI mice, mainly localizing to the mitochondrial of renal tubular cells, and discovered the increased serum levels of ARG2 in CI-AKI patients. ARG2-targeted inhibition or deficiency could dramatically attenuate renal dysfunction and tissue injury, reduce nitrosative stress and apoptosis of renal tubular cells during CI-AKI. What's more, similar results were found in the other two clinical commonly used drugs, cisplatin and vancomycin, induced AKI models. In terms of mechanism, upregulated ARG2 mediates

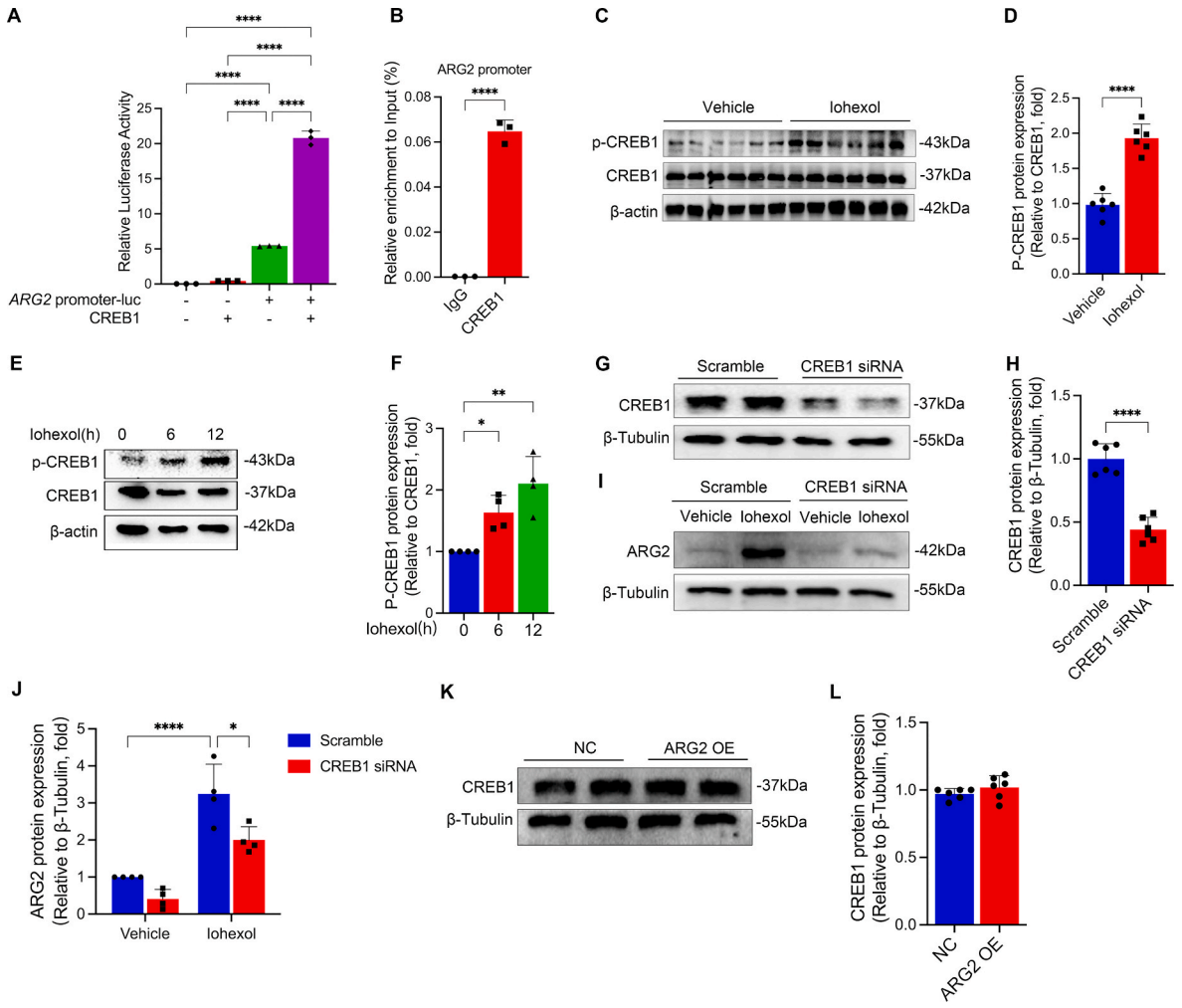

Fig. 8. CREB1 regulates ARG2 transcription. (A) Luciferase reporter gene results demonstrated that CREB1 combined with ARG2 promoter. (B) ChIP-PCR showed a direct combination and enrichment of CREB1 to the promoter region of ARG2. (C and D) The P-CREB1 and CREB1 protein expressions were evaluated in mice treated with iohexol. (E and F) The P-CREB1 and CREB1 protein expressions were evaluated in HK-2 cells cultured with iohexol at the indicated time points. (G–J) The CREB1 and ARG2 protein expression were evaluated in HK-2 cells transfected with CREB1 siRNA. (K and L) The CREB1 protein expression was evaluated in HK-2 cells transfected with ARG2 overexpression plasmid. $^{*}P < 0.05$, $^{**}P < 0.01$, $^{****}P < 0.0001$. mean ± SD, n = 6 in mice, n = 3-6 in HK-2 cells.

nitrosative stress and apoptosis of renal tubules, partially by decreasing HO-1 expression, then inducing CI-AKI, and CREB1 may be a transcription factor of ARG2.

To identify key target genes of CI-AKI, we used both proteomic and transcriptomic approaches [32] to determine the differentially expressed mRNA and protein in the renal tissues of iohexol-induced AKI mice, and discovered that both mRNA and protein expressions of ARG2 were dramatically increased. In an iohexol-induced AKI rat model, Deng et al. performed a proteomic investigation and identified 16 candidate proteins [35]. Kilari et al. employed RNA-Seq to investigate the impact of terazosin suppression of alpha-adrenergic receptor 1b on gene and protein expression in iohexol-induced AKI mouse, and found 436 down-regulated genes and 21 up-regulated genes [36]. Yet, ARG2 was not enriched in above mentioned studies. Of interest was that, in present study, not only iohexol-induced AKI mice but also cisplatin- and vancomycin-induced AKI mice had much higher mRNA and protein expressions of ARG2 in kidneys than control group, which has not yet been documented. To the best of our knowledge, we are the first to confirm the accumulation of ARG2 in the kidneys of iohexol-, cisplatin-, or vancomycin-induced AKI models.

ARG2, a subtype of arginase, hydrolyzes L-arginine to produce L-ornithine and urea [37]. ARG2 mRNA and protein are reported to be abundantly expressed in the renal tubules, especially in S3 section of the proximal tubules, of deep cortex and the outer medulla layer [18,25,38]. Similar to this, our immunofluorescence findings demonstrated that ARG2, particularly at the cortical and medullary junction, was considerably increased in renal tubules during CI-AKI. Furthermore, ARG2 colocalized with mitochondria, as shown in present study. ARG2's colocalization with mitochondria was diminished as a result of the partial mitochondrial rupture caused by the iohexol intervention. However, the role of ARG2 in kidney injury is still controversial. In the IRI model, the histological damage of ischemic kidney in ARG2 renal tubular epithelial knockout mice was more obvious and increased TUNEL-positive areas were found after IRI when compared with controls [25]. In contrast, Hara et al. found that ARG2 KO reduced IRI-induced abnormal renal function and acute tubular necrosis in mice, with reduced proportion of TUNEL-positive cells [23]. Selective inhibition of ARG2 can effectively prevent and improve diabetic kidney damage [22,39]. ARG2 silencing has protective effect on podocytes under hypoxia condition [40]. In present study, results showed that ARG2 KO significantly alleviated kidney injury in iohexol-, cisplatin-, and vancomycin-induced AKI mice via inhibiting apoptosis in renal tubular cells. The mechanism of ARG2 caused apoptosis may be through promoting nitrosative stress, which has been reported recently in mice with IRI [23] or bleomycin-induced pulmonary hypertension [41]. Similarly, our results showed that ARG2 KO or silencing could significantly

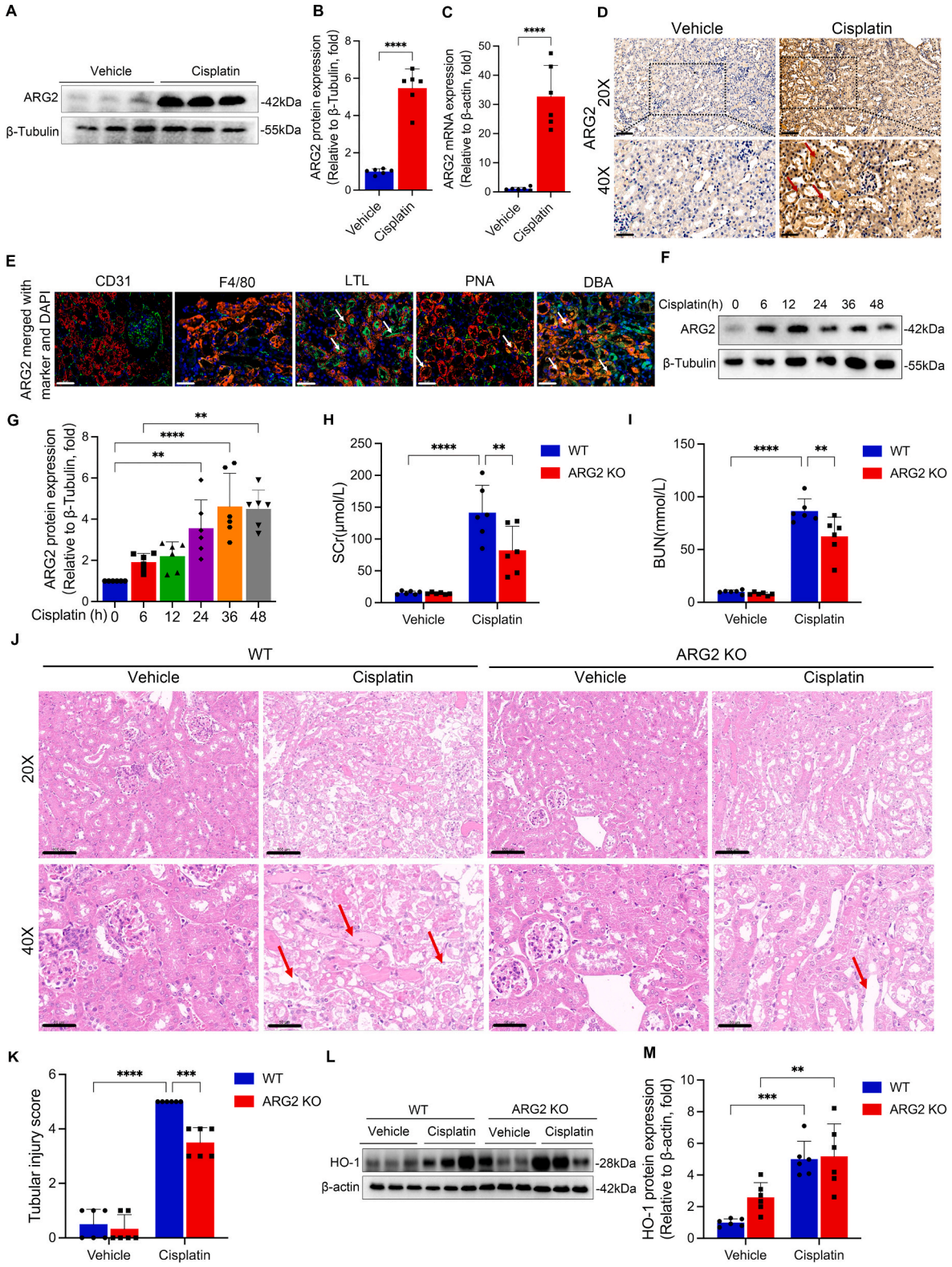

Fig. 9. ARG2 may be a potential target of cisplatin-induced AKI. (A–C) ARG2 protein and mRNA expressions in the kidneys of cisplatin-induced AKI mice. (D) Representative images of immunohistochemistry staining of ARG2 in cisplatin-induced AKI mice kidneys. The red arrows indicate deeper ARG2-positive staining of renal tubules. Scale, 20×, 100 μm, 40×, 50 μm. (E) Representative images of the immunofluorescence colocalization of CD31, F4/80, LTL, PNA, and DBA with ARG2 in the kidney of cisplatin-induced AKI mice. The following specific markers were used: endothelial, CD31; macrophage, F4/80; proximal tubule, lotus tetragonolobus lectin (LTL); distal tubule, peanut agglutinin (PNA); and collecting duct, dolichos biflorus agglutinin (DBA). The white arrows indicate positive tubules with colocalization of ARG2 and specific tubular markers. Scale, 50 μm. (F and G) ARG2 protein expression in primary tubular epithelial cells treated by cisplatin. (H–K) Renal function and renal tissue injury of ARG2 KO and WT mice administrated with cisplatin were assessed by SCr, BUN, and tubular injury score. The red arrows showed the vacuolar degeneration, tubular necrosis, cast formation, and tubular dilation of renal tubules. (L and M) The HO-1 protein expression was evaluated by western blotting in ARG2 KO and WT mice administrated with cisplatin. $^{*}P < 0.05$, $^{**}P < 0.01$, $^{***}P < 0.001$, $^{****}P < 0.0001$. mean ± SD, n = 6.

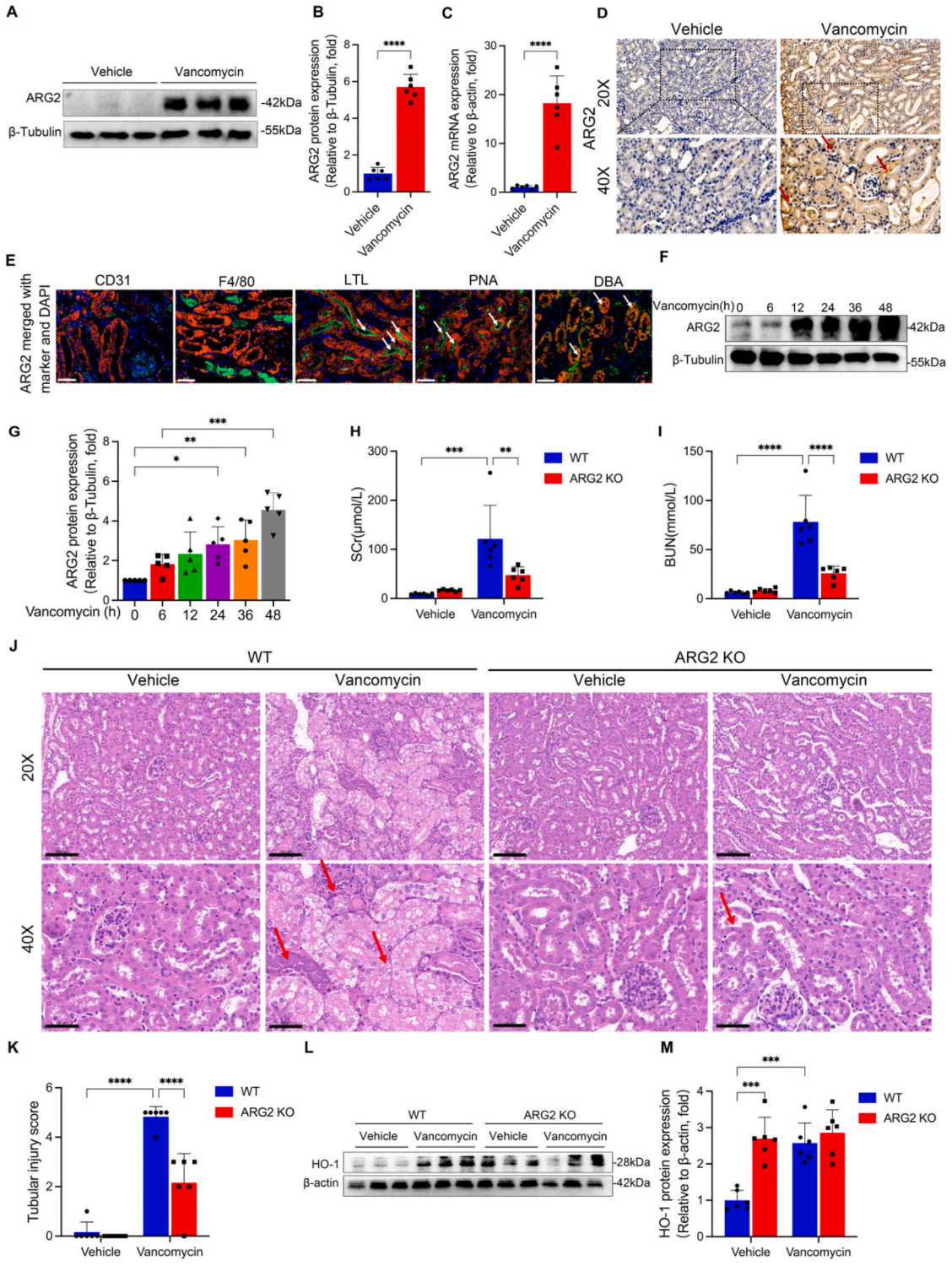

Fig. 10. ARG2 may be a potential target of vancomycin-induced AKI. (A–C) ARG2 protein and mRNA expressions in the kidneys of vancomycin-induced AKI mice. (D) Representative images of immunohistochemistry staining of ARG2 in vancomycin-induced AKI mice kidneys. The red arrows indicate deeper ARG2-positive staining of renal tubules. Scale, 20×, 100 μm, 40×, 50 μm. (E) Representative images of the immunofluorescence colocalization of CD31, F4/80, LTL, PNA, and DBA with ARG2 in the kidney of vancomycin-induced AKI mice. The following specific markers were used: endothelial, CD31; macrophage, F4/80; proximal tubule, lotus tetragonolobus lectin (LTL); distal tubule, peanut agglutinin (PNA); and collecting duct, dolichos biflorus agglutinin (DBA). The white arrows indicate positive tubules with colocalization of ARG2 and specific tubular markers. Scale, 50 μm. (F and G) ARG2 protein expression in primary tubular epithelial cells treated by vancomycin. (H–K) Renal function and renal tissue injury of ARG2 KO and WT mice administrated with vancomycin were assessed by SCr, BUN, and tubular injury score. The red arrows showed the vacuolar degeneration, tubular necrosis, cast formation, and tubular dilation of renal tubules. (L and M) The HO-1 protein expression was evaluated by western blotting in ARG2 KO and WT mice administrated with vancomycin. $^{*}P < 0.05$, $^{**}P < 0.01$, $^{***}P < 0.001$, $^{****}P < 0.0001$. mean ± SD, n = 6.

improve the nitrosative stress of renal tubular cells induced by iohexol, cisplatin or vancomycin.

After examining the correlations between all differentially expressed proteins measured by proteomics of kidney tissues in the iohexol induced AKI group compared with the control group, using the method similar with previous study [32], HO-1 was demonstrated to have a significantly negative correlation with ARG2 in present study. HO-1, an inducible cell protective enzyme, could degrade toxic free heme including hemoglobin, myoglobin, and cytochrome. Upon injury, toxic heme becomes unstable and release free heme, leading to oxidative stress, inflammation, and apoptosis [42]. Currently, several studies have demonstrated the protective effects of HO-1 in various AKI models, including glycerol [43], IRI [44], cisplatin [45], and lipopolysaccharide [46]. In those injury models [43–46], HO-1 protein expressions are all induced to prevent kidney failure *in vivo*. Similarly, in present study, we found upregulated expression of HO-1 in the kidneys, which may be a self-protection mechanism to protect against iohexol-induced AKI in mice. However, inconsistent with *in vivo* experiments, the decreased HO-1 mRNA and protein expressions were found in the *in vitro* experiments. ARG2 silencing could increase the mRNA and protein levels of HO-1, while HO-1 silencing or activating could not alter ARG2 protein expression. CHX results showed that ARG2 had no significant effect on the degradation of HO-1. HO-1 is a Nrf2-targeted gene, and a recent study reports that Nrf2 activation is reduced in ARG2 knockout in UUO kidneys [47], which may be the potential mechanism involved in ARG2 regulated HO-1 expression. These results indicated that the ARG2 may down-regulate the transcription of HO-1, contributing to a deeper understanding of various physiological and pathological processes involved in HO-1.

It has been reported that ARG2 transcription factors include HIF-2 [48] and interferon regulatory factor 3 (IRF3) [49]. We demonstrated the binding of CREB1 to the ARG2 promoter by luciferase reporter gene assay and CHIP analysis, and then upregulating ARG2 expression. CREB1 is a key transcription factor mediating transcriptional responses to a variety of growth factors and stress signals [50]. Barra et al. found that apoptotic cells derived factors activated ERK5 and CREB induced anti-inflammatory macrophage phenotype through ARG2, and CREB induced ARG2 expression [51], which is consistent with present study.

There are some limitations of this study. First of all, we only studied the effect of ARG2 in three AKI models: iohexol, cisplatin and vancomycin. However, there are other drugs that can cause AKI, and further studies should be conducted regarding the effect of ARG2 on other drug induced AKI models. Second, only whole-body ARG2 knockout mice were constructed. Although ARG2 was mainly expressed in renal tubules of CI-AKI mice, it could not be ruled out whether ARG2 in other parts caused by whole-body knockout did indeed participate in the protective effect of CI-AKI. Third, we demonstrated that ARG2 regulates HO-1 expression by regulating its transcription, rather than by inhibiting degradation. However, the specific mechanism of action has not been fully studied, and further research is needed to explore its specific regulatory mechanism.

5. Conclusions

In summary, our study suggests that ARG2 is a key target of CI-AKI. ARG2 deletion can improve CI-AKI by reducing nitrosative stress and apoptosis of renal tubular cells, partially by up-regulating HO-1 expression. And the transcription of ARG2 may be regulated by the CREB1. Similar results were found in the other two clinical commonly used drugs, cisplatin and vancomycin, induced AKI models. These findings may provide new insights into the pathogenesis of CI-AKI, even drug induced AKI, and strategies for its prevention and treatment.

Author contributions

Ling-yun Zhou, Kun Liu, and Xiao-cong Zuo conceived the study and designed the experiments. Ling-yun Zhou and Kun Liu performed the main experiments and analyzed data. Wen-jun Yin, Zhi-yao Tang, Yue-liang Xie, Jiang-lin Wang, Shan-ru Zuo and Yi-feng Wu participated in some experiments. Ling-yun Zhou and Kun Liu wrote the manuscript. Xiao-cong Zuo revised the manuscript. All authors have approved the final article for publication.

Declaration of competing interest

Authors declare that there are no conflicts of interest.

Acknowledgments

This study was supported by National Natural Science Foundation of China (No.U22A20386, China), National Natural Science Foundation of China (No.81973400, China), National Natural Science Foundation of China (No.82104305, China), Hunan Provincial Natural Science Foundation of China (No.2021JJ40957, China), Hunan Engineering Research Center of Intelligent Prevention and Control for Drug Induced Organ Injury (No.40, China), Research and Development Plan of Key Areas of Science and Technology Innovation in Hunan Province (No.2022SK2021, China), the Science and Technology Innovation Program of Hunan Province (No.2023RC1032, China).

Appendix A. Supplementary data

Supplementary data to this article can be found online at https://doi.org/10.1016/j.redox.2023.102929.

References

[1] L. Yang, G. Xing, L. Wang, Y. Wu, S. Li, G. Xu, Q. He, J. Chen, M. Chen, X. Liu, Z. Zhu, L. Yang, X. Lian, F. Ding, Y. Li, H. Wang, J. Wang, R. Wang, C. Mei, J. Xu, R. Li, J. Cao, L. Zhang, Y. Wang, J. Xu, B. Bao, B. Liu, H. Chen, S. Li, Y. Zha, Q. Luo, D. Chen, Y. Shen, Y. Liao, Z. Zhang, X. Wang, K. Zhang, L. Liu, P. Mao, C. Guo, J. Li, Z. Wang, S. Bai, S. Shi, Y. Wang, J. Wang, Z. Liu, F. Wang, D. Huang, S. Wang, S. Ge, Q. Shen, P. Zhang, L. Wu, M. Pan, X. Zou, P. Zhu, J. Zhao, M. Zhou, L. Yang, W. Hu, J. Wang, B. Liu, T. Zhang, J. Han, T. Wen, M. Zhao, H. Wang, Acute kidney injury in China: a cross-sectional survey, Lancet 386 (10002) (2015) 1465–1471.

[2] J. Bejoy, E.S. Qian, L.E. Woodard, Tissue culture models of AKI: from tubule cells to human kidney organoids, J. Am. Soc. Nephrol. 33 (3) (2022) 487–501.

[3] M.T. James, M. Bhatt, N. Pannu, M. Tonelli, Long-term outcomes of acute kidney injury and strategies for improved care, Nat. Rev. Nephrol. 16 (4) (2020) 193–205.

[4] C. Liu, S. Yan, Y. Wang, J. Wang, X. Fu, H. Song, R. Tong, M. Dong, W. Ge, J. Wang, H. Yang, C. Wang, P. Xia, L. Zhao, S. Shen, J. Xie, Y. Xu, P. Ma, H. Li, S. Lu, Y. Ding, L. Jiang, Y. Lin, M. Wang, F. Qiu, W. Feng, L. Yang, Drug-induced hospital-acquired acute kidney injury in China: a multicenter cross-sectional survey, Kidney Dis. 7 (2) (2021) 143–155.

[5] H. Wang, T. Gao, R. Zhang, J. Hu, Y. Wang, J. Wei, Y. Zhou, H. Dong, The intellectual base and global trends in contrast-induced acute kidney injury: a bibliometric analysis, Ren. Fail. 45 (1) (2023), 2188967.

[6] R. Morcos, M. Kucharik, P. Bansal, H. Al Taii, R. Manam, J. Casale, H. Khalili, B. Maini, Contrast-induced acute kidney injury: review and practical update, Clin. Med. Insights Cardiol. 13 (2019), 1179546819878680.

[7] K. Nash, A. Hafeez, S. Hou, Hospital-acquired renal insufficiency, Am. J. Kidney Dis. 39 (5) (2002) 930–936.

[8] L. Azzalini, V. Spagnoli, H.Q. Ly, Contrast-induced nephropathy: from pathophysiology to preventive strategies, Can. J. Cardiol. 32 (2) (2016) 247–255.

[9] M.A. Perazella, Drug-induced acute kidney injury: diverse mechanisms of tubular injury, Curr. Opin. Crit. Care 25 (6) (2019) 550–557.

[10] M. Fontecha-Barriuso, A.M. Lopez-Diaz, J. Guerrero-Mauvecin, V. Miguel, A. M. Ramos, M.D. Sanchez-Nino, M. Ruiz-Ortega, A. Ortiz, A.B. Sanz, Tubular mitochondrial dysfunction, oxidative stress, and progression of chronic kidney disease, Antioxidants 11 (7) (2022) 1356.

[11] Q. Lin, S. Li, N. Jiang, X. Shao, M. Zhang, H. Jin, Z. Zhang, J. Shen, Y. Zhou, W. Zhou, L. Gu, R. Lu, Z. Ni, PINK1-parkin pathway of mitophagy protects against contrast-induced acute kidney injury via decreasing mitochondrial ROS and NLRP3 inflammasome activation, Redox Biol. 26 (2019), 101254.

[12] Q. Lin, S. Li, N. Jiang, H. Jin, X. Shao, X. Zhu, J. Wu, M. Zhang, Z. Zhang, J. Shen, W. Zhou, L. Gu, R. Lu, Z. Ni, Inhibiting NLRP3 inflammasome attenuates apoptosis in contrast-induced acute kidney injury through the upregulation of HIF1A and BNIP3-mediated mitophagy, Autophagy 17 (10) (2021) 2975–2990.

[13] S.B. Duan, S.K. Yang, Q.Y. Zhou, P. Pan, H. Zhang, F. Liu, X.Q. Xu, Mitochondria-targeted peptides prevent on contrast-induced acute kidney injury in the rats with hypercholesterolemia, Ren. Fail. 35 (8) (2013) 1124–1129.

[14] S. Huang, Y. Tang, T. Liu, N. Zhang, X. Yang, D. Yang, G. Hong, A novel antioxidant protects against contrast medium-induced acute kidney injury in rats, Front. Pharmacol. 11 (2020), 599577.
[15] X.F. Guan, Q.J. Chen, X.C. Zuo, R. Guo, X.D. Peng, J.L. Wang, W.J. Yin, D.Y. Li, Contrast media-induced renal inflammation is mediated through HMGB1 and its receptors in human tubular cells, DNA Cell Biol. 36 (1) (2017) 67–76.
[16] C. Hu, G. Zhou, K. Liu, W. Yin, L. Zhou, J. Wang, L. Chen, S. Zuo, Y. Xie, X. Zuo, CaMKII as a key regulator of contrast-induced nephropathy through mPTP opening in HK-2 cells, Cell. Signal. 75 (2020), 109734.
[17] R.W. Caldwell, P.C. Rodriguez, H.A. Toque, S.P. Narayanan, R.B. Caldwell, Arginase: a multifaceted enzyme important in health and disease, Physiol. Rev. 98 (2) (2018) 641–665.
[18] O. Levillain, S. Balvay, S. Peyrol, Localization and differential expression of arginase II in the kidney of male and female mice, Pflügers Archiv 449 (5) (2005) 491–503.
[19] G. Wu, S.M. Morris Jr., Arginine metabolism: nitric oxide and beyond, Biochem. J. 336 (1998) 1–17. Pt 1)(Pt 1.
[20] J.L. Deignan, S.D. Cederbaum, W.W. Grody, Contrasting features of urea cycle disorders in human patients and knockout mouse models, Mol. Genet. Metabol. 93 (1) (2008) 7–14.
[21] O. Shi, S.M. Morris Jr., H. Zoghbi, C.W. Porter, W.E. O'Brien, Generation of a mouse model for arginase II deficiency by targeted disruption of the arginase II gene, Mol. Cell Biol. 21 (3) (2001) 811–813.
[22] H. You, T. Gao, T.K. Cooper, S.M. Morris Jr., A.S. Awad, Arginase inhibition mediates renal tissue protection in diabetic nephropathy by a nitric oxide synthase 3-dependent mechanism, Kidney Int. 84 (6) (2013) 1189–1197.
[23] M. Hara, K. Torisu, K. Tomita, Y. Kawai, K. Tsuruya, T. Nakano, T. Kitazono, Arginase 2 is a mediator of ischemia-reperfusion injury in the kidney through regulation of nitrosative stress, Kidney Int. 98 (3) (2020) 673–685.
[24] Y. Uchida, K. Torisu, S. Aihara, N. Imazu, H. Ooboshi, T. Kitazono, T. Nakano, Arginase 2 promotes cisplatin-induced acute kidney injury by the inflammatory response of macrophages, Lab. Invest. 103 (10) (2023), 100227.
[25] C. Ansermet, G. Centeno, S. Lagarrigue, S. Nikolaeva, H.A. Yoshihara, S. Pradervand, J.L. Barras, N. Dattner, S. Rotman, F. Amati, D. Firsov, Renal tubular arginase-2 participates in the formation of the corticomedullary urea gradient and attenuates kidney damage in ischemia-reperfusion injury in mice, Acta Physiol. 229 (3) (2020), e13457.
[26] L.S. Chawla, R. Bellomo, A. Bihorac, S.L. Goldstein, E.D. Siew, S.M. Bagshaw, D. Bittleman, D. Cruz, Z. Endre, R.L. Fitzgerald, L. Forni, S.L. Kane-Gill, E. Hoste, J. Koyner, K.D. Liu, E. Macedo, R. Mehta, P. Murray, M. Nadim, M. Ostermann, P. M. Palevsky, N. Pannu, M. Rosner, R. Wald, A. Zarbock, C. Ronco, J.A. Kellum, Acute disease quality initiative W. Acute kidney disease and renal recovery: consensus report of the acute disease quality initiative (ADQI) 16 workgroup, Nat. Rev. Nephrol. 13 (4) (2017) 241–257.
[27] X. Fan, X. Zhang, L.C. Liu, S. Zhang, C.B. Pelger, H.Y. Lughmani, S.T. Haller, W. T. Gunning 3rd, C.J. Cooper, R. Gong, L.D. Dworkin, R. Gupta, Hemopexin accumulates in kidneys and worsens acute kidney injury by causing hemoglobin deposition and exacerbation of iron toxicity in proximal tubules, Kidney Int. 102 (6) (2022) 1320–1330.
[28] J. Li, X. Sun, N. Yang, J. Ni, H. Xie, H. Guo, X. Wang, L. Zhou, J. Liu, S. Chen, X. Wang, Y. Zhang, C. Yu, W. Zhang, L. Lu, Phosphoglycerate mutase 5 initiates inflammation in acute kidney injury by triggering mitochondrial DNA release by dephosphorylating the pro-apoptotic protein Bax, Kidney Int. 103 (1) (2023) 115–133.
[29] Y. Xu, H. Ma, J. Shao, J. Wu, L. Zhou, Z. Zhang, Y. Wang, Z. Huang, J. Ren, S. Liu, X. Chen, J. Han, A role for tubular necroptosis in cisplatin-induced AKI, J. Am. Soc. Nephrol. 26 (11) (2015) 2647–2658.
[30] K. Liu, C. Hu, W. Yin, L. Zhou, X. Gu, X. Zuo, An in vivo and in vitro model on the protective effect of cilnidipine on contrast-induced nephropathy via regulation of apoptosis and CaMKII/mPTP pathway, J. Biochem. Mol. Toxicol. 37 (1) (2023), e23238.
[31] Y.X. Deng, K. Liu, Q.X. Qiu, Z.Y. Tang, R.M. Que, D.K. Li, X.R. Gu, G.L. Zhou, Y. F. Wu, L.Y. Zhou, W.J. Yin, X.C. Zuo, Identification and validation of hub genes in drug induced acute kidney injury basing on integrated transcriptomic analysis, Front. Immunol. 14 (2023), 1126348.
[32] P. Simic, W. Kim, W. Zhou, K.A. Pierce, W. Chang, D.B. Sykes, N.B. Aziz, S. Elmariah, D. Ngo, P.D. Pajevic, N. Govea, B.R. Kestenbaum, I.H. de Boer, Z. Cheng, M. Christov, J. Chun, D.E. Leaf, S.S. Waikar, A.M. Tager, R.E. Gerszten, R.I. Thadhani, C.B. Clish, H. Juppner, M.N. Wein, E.P. Rhee, Glycerol-3-phosphate is an FGF23 regulator derived from the injured kidney, J. Clin. Invest. 130 (3) (2020) 1513–1526.
[33] M.A. Perazella, M.H. Rosner, Drug-induced acute kidney injury, Clin. J. Am. Soc. Nephrol. 17 (8) (2022) 1220–1233.
[34] F. Li, X. Sun, B. Zheng, K. Sun, J. Zhu, C. Ji, F. Lin, L. Huan, X. Luo, C. Yan, J. Xu, Y. Hong, Y. Wang, X. Xu, J. Sun, Z. Song, F. Kong, J. Shi, Arginase II promotes intervertebral disc degeneration through exacerbating senescence and apoptosis caused by oxidative stress and inflammation via the NF-kappaB pathway, Front. Cell Dev. Biol. 9 (2021), 737809.
[35] Y.H. Deng, X.F. Wang, X. Wu, P. Yan, Q. Liu, T. Wu, S.B. Duan, Differential renal proteomics analysis in a novel rat model of iodinated contrast-induced acute kidney injury, Ren. Fail. 45 (1) (2023), 2178821.
[36] S. Kilari, A. Sharma, C. Zhao, A. Singh, C. Cai, M. Simeon, A.J. van Wijnen, S. Misra, Identification of novel therapeutic targets for contrast induced acute kidney injury (CI-AKI): alpha blockers as a therapeutic strategy for CI-AKI, Transl. Res. 235 (2021) 32–47.
[37] C. De Santi, F.K. Nally, R. Afzal, C.P. Duffy, S. Fitzsimons, S.L. Annett, T. Robson, J. K. Dowling, S.A. Cryan, C.E. McCoy, Enhancing arginase 2 expression using target site blockers as a strategy to modulate macrophage phenotype, Mol. Ther. Nucleic Acids 29 (2022) 643–655.
[38] O. Levillain, A. Hus-Citharel, S. Garvi, S. Peyrol, I. Reymond, M. Mutin, F. Morel, Ornithine metabolism in male and female rat kidney: mitochondrial expression of ornithine aminotransferase and arginase II, Am. J. Physiol. Ren. Physiol. 286 (4) (2004) F727–F738.
[39] S.M. Morris Jr., H. You, T. Gao, J. Vacher, T.K. Cooper, A.S. Awad, Distinct roles of arginases 1 and 2 in diabetic nephropathy, Am. J. Physiol. Ren. Physiol. 313 (4) (2017) F899–F905.
[40] Z. Ren, D.M. Potenza, Y. Ma, G. Ajalbert, D. Hoogewijs, X.F. Ming, Z. Yang, Role of arginase-II in podocyte injury under hypoxic conditions, Biomolecules 12 (9) (2022).
[41] B.H. Koo, M.H. Won, Y.M. Kim, S. Ryoo, p32-Dependent p38 MAPK activation by arginase II downregulation contributes to endothelial nitric oxide synthase activation in HUVECs, Cells 9 (2) (2020).
[42] M.J. Tracz, J. Alam, K.A. Nath, Physiology and pathophysiology of heme: implications for kidney disease, J. Am. Soc. Nephrol. 18 (2) (2007) 414–420.
[43] K.A. Nath, G. Balla, G.M. Vercellotti, J. Balla, H.S. Jacob, M.D. Levitt, M. E. Rosenberg, Induction of heme oxygenase is a rapid, protective response in rhabdomyolysis in the rat, J. Clin. Invest. 90 (1) (1992) 267–270.
[44] H. Shimizu, T. Takahashi, T. Suzuki, A. Yamasaki, T. Fujiwara, Y. Odaka, M. Hirakawa, H. Fujita, R. Akagi, Protective effect of heme oxygenase induction in ischemic acute renal failure, Crit. Care Med. 28 (3) (2000) 809–817.
[45] A. Agarwal, J. Balla, J. Alam, A.J. Croatt, K.A. Nath, Induction of heme oxygenase in toxic renal injury: a protective role in cisplatin nephrotoxicity in the rat, Kidney Int. 48 (4) (1995) 1298–1307.
[46] M.J. Tracz, J.P. Juncos, J.P. Grande, A.J. Croatt, A.W. Ackerman, G. Rajagopalan, K.L. Knutson, A.D. Badley, M.D. Griffin, J. Alam, K.A. Nath, Renal hemodynamic, inflammatory, and apoptotic responses to lipopolysaccharide in HO-1-/- mice, Am. J. Pathol. 170 (6) (2007) 1820–1830.
[47] S. Aihara, K. Torisu, Y. Uchida, N. Imazu, T. Nakano, T. Kitazono, Spermidine from arginine metabolism activates Nrf2 and inhibits kidney fibrosis, Commun. Biol. 6 (1) (2023) 676.
[48] K. Krotova, J.M. Patel, E.R. Block, S. Zharikov, Hypoxic upregulation of arginase II in human lung endothelial cells, Am. J. Physiol. Cell Physiol. 299 (6) (2010) C1541–C1548.
[49] N. Grandvaux, F. Gaboriau, J. Harris, B.R. tenOever, R. Lin, J. Hiscott, Regulation of arginase II by interferon regulatory factor 3 and the involvement of polyamines in the antiviral response, FEBS J. 272 (12) (2005) 3120–3131.
[50] Y.W. Wang, X. Chen, R. Ma, P. Gao, Understanding the CREB1-miRNA feedback loop in human malignancies, Tumour Biol. 37 (7) (2016) 8487–8502.
[51] V. Barra, A.M. Kuhn, A. von Knethen, A. Weigert, B. Brune, Apoptotic cell-derived factors induce arginase II expression in murine macrophages by activating ERK5/CREB, Cell. Mol. Life Sci. 68 (10) (2011) 1815–1827.